

Brain Tumor Augmentation Using the U-NET Architecture



Author
Mohsin Jabbar
NUST CEME 00000205570

Supervisor
Dr. Farhan Hussain
Co- Supervisor
Dr. Sultan Daud Khan

DEPARTMENT OF COMPUTER ENGINEERING
COLLEGE OF ELECTRICAL & MECHANICAL ENGINEERING
NATIONAL UNIVERSITY OF SCIENCES AND TECHNOLOGY
ISLAMABAD

April, 2021

Brain Tumor Augmentation Using the U-NET Architecture

Author

Mohsin Jabbar
NUST CEME 00000205570

A thesis submitted in partial fulfillment of the requirements for the degree of
MS Computer Engineering

Thesis Supervisor

Dr. FARHAN HUSSAIN

Thesis Supervisor's Signature: _____

DEPARTMENT OF COMPUTER ENGINEERING
COLLEGE OF ELECTRICAL & MECHANICAL ENGINEERING
NATIONAL UNIVERSITY OF SCIENCES AND TECHNOLOGY
ISLAMABAD

July, 2021

Declaration

I declare that this research paper titled “Brain tumor augmentation using the U-NET architecture” has been solely the result of my own work. And the content that is taken from other sources has been properly acknowledged/referred by them. And the work presented herein has not been submitted anywhere else for assessment

Signature of Student

Mohsin Jabbar

NUST CEME 00000205570

Language Correctness Certificate

This thesis is approved by an English expert in terms of language and therefore, it is all type of error free including typing, syntax, semantics, grammatical and spelling mistakes. Also, while doing this thesis, proper format given by the university is strictly followed.

Signature of Student

Mohsin Jabbar

NUST CEME 00000205570

Signature of Supervisor

Dr. FARHAN HUSSAIN

Copyright Statement

- Copyright in this thesis' text is vested to the student's author. Copies (by any process) either full or extract ones, are made only as per the instructions given by the author as well as lodged in the Library of NUST College of E&ME. Details could be obtained by the Librarian. This page must form the part of any such copies made. Further copies (by any process) are not allowed without the permission (in writing) of the author.
- The ownership of any intellectual property described in the thesis belongs to NUST College of E&ME, subject to any prior agreement to the contrary, and is not available for any third party to use it without the written permission of the College of E&ME. And the mentioned institute will direct the terms and conditions of any such agreement if made.
- Moreover, information on the conditions under which disclosures and exploitation may take place is available from the Library of NUST College of E&ME, Rawalpindi.

Acknowledgements

I am highly grateful to Almighty Allah to give me the courage, guided me at every step throughout this work, and to bless me with new ideas to make my work more effective and creative. Without HIS support I was unable to write even a single new idea. The other people who helped me out during this thesis work was also just because of Allah Almighty will WHO brought such nice people in my life. So, indeed none be worthy of praise but You (ALLAH).

I am also thankful to my beloved parents who nurtured me in a way to be able to do something good and continued to support and guide me throughout my life.

I would also like to say heartiest thanks to my beloved supervisor DR. FARHAN HUSSAIN for his generous behavior and cooperation throughout my thesis and also for Machine Learning and Operating System courses which he taught me. I can surely say that I have not such a great command over any other engineering subject like the ones which taught.

I would also express my special thanks to DR. USMAN AKRAM for his tremendous support and help whenever the need arose. He always get me out from the problems whenever I got stuck. Without him, I was not able to do this thesis ever..

I am also thankful to DR. ARSALAN SHAUKAT and DR. WASI HAIDER BUTT for their guidance and support and evaluation committee and express my special Thanks to Muhammad SADAM HUSSAIN for his help.

At the end, I would like to convey my regards and respect to all those who have rendered their valuable assistance to my thesis work.

Mohsin Jabbar

*To my beloved, Proud Parents since I owe all my success to you! Thanks
a bunch!*

Abstract

Studies have found out that tumors in brain are one of the fiercest diseases which can ultimately lead to death. Gliomas are the most commonly found primary tumors that are very hard to predict and can be found anywhere in the brain. It is prime objective to differentiate the different tumor tissues such as enhancing tissues, edema, from healthy ones. To do this task, two types of segmentation techniques come into existent i.e. manual and automatic. The automation methods of brain tumor segmentation have gained ground over manual segmentation algorithms and further its estimation is very closer to clinical results. In this paper we propose a comprehensive U-NET architecture with modification in their layers for 2D slices segmentation as a major contribution to BRATS 2015 challenge.. Then we enlisted different datasets that are available publicly i.e. BRATS and DICOM. Further, we present a robust framework inspired from U-NET model with addition and modification of layers and image pre-processing methodology such as contrast enhancement for visible input and output details. In this way our approach achieves highest dice score 0.92 on the publicly available BRATS 2015 dataset and with better time constraint i.e. training time decreases to 80-90 minute instead of previously 2 to 3 days. We put our approach to the test on the benchmark brats 2015 dataset, and it outperformed the competition in terms of performance and Dice Score.

Keywords— DICOM, Segmentation, U-NET, Gliomas, BRATS 2015

Table of Contents

| | |
|---|------|
| Declaration..... | iii |
| Language Correctness Certificate | ii |
| Copyright Statement | ii |
| Acknowledgements..... | iiiv |
| Abstract..... | v |
| List of Figures..... | vi |
| List of Tables | vii |
| Chapter 1: Introduction..... | 11 |
| 1.1 Brief Description and Motivation | 111 |
| 1.2 Types of Brain Imaging Methods | 13 |
| 1.3 Brain Tumor Segmentation and its Types | 134 |
| 1.4 Research Challenge and Contribution | 145 |
| 1.5 Aims of the Thesis | 156 |
| 1.6 Circumscription..... | 166 |
| 1.7 Structure of the Thesis | 166 |
| Chapter 2: Related Background | 177 |
| 2.1 Tumor..... | 177 |
| 2.2 Brain Tumors Scans..... | 177 |
| 2.3 Conventional Image Processing Approaches..... | 178 |
| 2.4 Primary Machine Learning Algorithm..... | 18 |
| 2.5 Clustering Techniques | 19 |
| 2.6 Convolution Neural Networks Approaches..... | 20 |
| 2.7 Dataset..... | 23 |
| 2.7.1 DICOM..... | 24 |
| 2.7.2 ISBR..... | 24 |
| 2.7.3 BRATS..... | 24 |
| 2.8 Challeneges and Problems | 26 |

| | |
|--|----|
| Chapter 3: Methodolgy | 27 |
| 3.1 Overview of overall Proposed Methodolgy | 27 |
| 3.2 Image preprocessing | 29 |
| 3.3 Formation of patches..... | 30 |
| 3.4 U-NET Framework For Brain Tumor Segmentation | 29 |
| 3.4.1 U-NET Architectural Detail | 31 |
| 3.4.2 Generic U-NET Archuitecture | 31 |
| 3.5 Proposed Modified U-NET Architecture | 32 |
| 3.5.1 Encoding left: Left Side Of the Architecture | 34 |
| 3.5.2 Decoding left: Right Side Of the Architecture | 36 |
| 3.6 Training..... | 37 |
| 3.7 Loss Function..... | 38 |
| 3.7.1 Optimization of Loss Function | 38 |
| 3.8 Batch Normalization | 38 |
| 3.4 DropOut Layers | 39 |
| 3.4 Network Training | 41 |
| Chapter 4: Experimental Results | 42 |
| 4.1 Dataset Description..... | 42 |
| 4.2 Implementation of robust U-NET architecture | 42 |
| 4.2.1 Designed Modified U-NET architecture..... | 43 |
| 4.3 Step By Step Training Mechanism | 43 |
| 4.4 Testing Mechanism..... | 43 |
| 4.5 Detail overview of hardware..... | 44 |
| 4.6 Fine tuning of hyper-parameter of U-NET architecture | 46 |
| 4.6.1 Neuronal Activation | 46 |
| 4.6.2 Loss Function Optimization | 47 |
| 4.6.3 Normalization | 47 |
| 4.6.4 Optimization Function..... | 47 |

| | |
|---|-------|
| 4.7 Comparative analysis of results | 47 |
| Chapter 5: Conclusion and Future Work | 49 |
| 5.1 Future Work | 49 |
| 5.1.1 Dataset | 49 |
| 5.2 Transfer Learning | 50 |
| References | 51-53 |

List of Figures

| | |
|---|-----|
| Figure 1. 1 Example of Example of Inner Brain Composition | 122 |
| Figure 1.2 Scans of MRI T1 T1C T2 T2FLAIR and Ground Truth from left to right in BRATS 2015 Dataset 14 | |
| Figure 1.3 before and After Segmentation of Brain MRI images | 15 |
| Figure 2.1 CNN Basic framework | 22 |
| Figure 2.2 Sub region of Glioma | 25 |
| Fig. 2.3 First four MRI scans are four MRI modalities and on the extreme right corner there is a ground truth. | 25 |
| Figure 3.1 Proposed Approach of training and testing algorithm | 28 |
| Figure 3.2 Block diagram of our proposed model..... | 29 |
| Figure 3.3 after image preprocessing results..... | 30 |
| Figure 3.4 Generic U-NET Architecture..... | 32 |
| Figure 3.5 Proposed Modified Tuned U-NET Architecture..... | 34 |
| Figure 3.7 Decoding working side | 37 |
| Figure 3.8 Training Kernel size | 38 |
| Figure 3.9 Batch Normalization | 39 |
| Figure 4.1 BRATS 2015 Dataset snap.... | 40 |
| Figure 4.2 Complete overview of Training mechanism..... | 44 |
| Figure4.3 Segmented output..... | 45 |
| Figure 4.4 Segmented output 2..... | 45 |
| Figure 4.2 Complete overview of Training mechanism..... | 44 |

List of Tables

| | |
|---|----|
| Table 2. 1 Advantages and disadvantage of various image processing method. | 20 |
| TABLE 3.1: DETAIL OF ALL THE ENCODING LAYERS | 35 |
| TABLE 3.2: DETAIL OF ALL THE DECODING LAYERS | 36 |
| TABLE 4.1 Comparative analysis using Dice score as performance evaluating of various brain tumor segmentation architectures | 48 |

Chapter 1: Introduction

1.1 Brief Description and Motivation

In medical imaging, segmentation and quantities assessment of tumors has a vital role to play. It is crucial for monitoring and planning of treatment strategies of the disease. These assessments can provide valuable knowledge about the spatial distribution of the lesions and their different types. Gliomas, on the other hand, are extremely difficult to segment because they are easily defused by their environment. They contrast poorly with aberrant or irregular structures. These tumors can also be detected anywhere in the brain and come in a variety of sizes, shapes ranging from tiny to enormous.

However, early detection of a Gliomas tumors is critical for better therapy and patient survival. However, due to the variability of tumors features among patients, automatic tumors segmentation has always been a difficult process. Some of the main explanations are low-intensity MRI pictures and irregular tumors forms. Now, with the improvements of machine learning due to technology, improvements have been shown in effective segmentation of these tumors. Advance convolutional neural network architectures have provided good classification results for various datasets.

Gliomas is the most common type of primary brain tumors. Gliomas tumors account for approximately 29% brain tumors, according to estimates. Gliomas tumors develop in glial cells. In the brain, these cells helps neurons a lot.. In the United States, approximately 16,000 new cases of gliomas were diagnosed in 2018[4].

Low-Grade Gliomas (LGG) and High-Grade Gliomas (HGG) are two types of gliomas (HGG). LGG accounts for approximately 28% of all new gliomas, and these are the early stages of the disease (stage 1 and stage 2). Advanced gliomas are classified as High-Grade gliomas (stages 3 and 4) and have a 70 percent occurrence rate. Glioma patients have a one-year survival rate of 37.2 percent, a five-year rate of 5.1 percent, and a ten-year rate of only 2.6 percent from the day of diagnosis, making it the most lethal of all cancer types.

It is also difficult to segment gliomas their surroundings quickly detonate them. They also contrast poorly with aberrant and irregular structures. Tumors of all sizes and shapes can be discovered anywhere in the brain. Early detection of a Glioma tumors is critical for better therapy. Before beginning treatment, a medical professional must determine which cells are healthy and which are malignant.

White matter, grey matter, and cerebrospinal fluid are the three types of healthy brain tissues (CSF). Tumorous brain regions consist of edema, necrotic tissues and active tumorous tissues. Normally, glioma tissues are diffused into healthy tissues in such a way that we hardly distinguish them from healthy tissues. The goal for the glioma brain tumor segmentation problem is to correctly segment the tumor infected tissues from the healthy and normal tissues. In case of a glioma brain tumor, accurate segmentation of regions is important because an estimation of the volumes of these sub-regions is crucial for planning and treatment follow up. Figure 1.1 Shows the tissue composition in human brain.

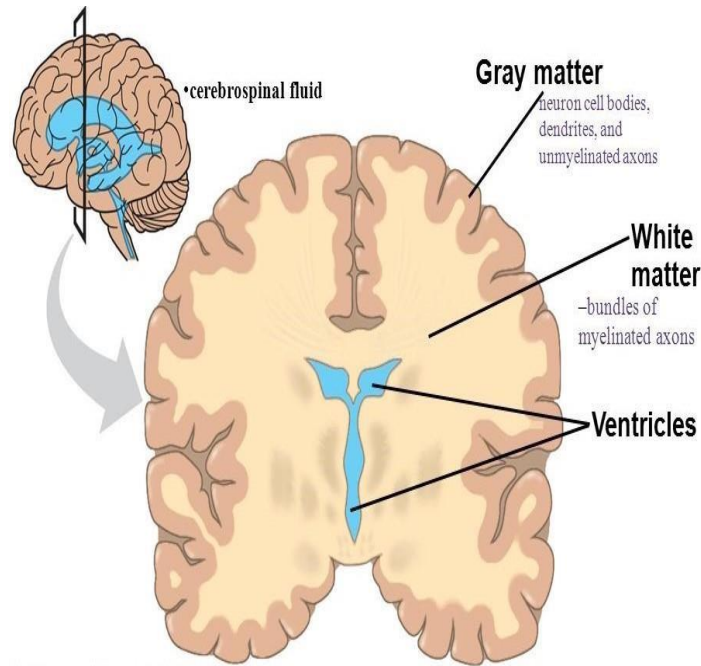


Figure 1. 1 Example of Inner Brain Composition.

Magnetic resonance imaging (MRI) is most accepted mechanism for brain tumor identification and recognition. Various MRI modalities make it more useful over other provided frameworks such as computed tomography (CT), positron emission tomography (PET) and magnetic resonance spectroscopy (MRS). Further, MRI image segmentation is pivotal in order to monitor the irregular shapes of tumors and it performs well in differentiating between healthy tissues and abnormal tissues. Moreover, gliomas 'complexity and subtle differences in MRI analysis create insurmountable challenges for radiologists' experts. This is so, because they cannot easily diagnose it by visual inspection of MRI. Modalities. Automation approach of brain tumor segmentation is most widely adopted mechanism for brain tumor classification. While, using these segmentation techniques for brain tumor, first MRI 3D images are converted into 2D slices. Later on they are divided into various classes for the ease of use [11]. Moving on, MRI modalities are combined to create multi model images. These images provide a detailed analysis of irregular formed tumors that are difficult to locate with a single modality. There are some modalities named as T1 (MRI), T1C (MRI with contrast improvement), T2 MRI, and T2-weighted MRI with fluid attenuated inversion recovery (T2) (T2-Flair) [9].

The human brain is divided into three zones i.e. white matter (WM), grey matter (GM), and cerebrospinal fluid (CSF). In surrounding of white matter (WM), tumor with unbounded boundaries are created and make it difficult to segment these regions. The swelling around the brain is created due to extreme tumors effects with their sub categories i.e. necrotic center, active tumor region, and edema. However, a precisely segmented tumor region is also of paramount importance in medical identifying and cure planning.

Recently a growing number in automation in brain segmentation approaches have been accepted widely inspired by deep neural networks. Presently, U-NET is one of the most influential deep neural network algorithms along with its encoding and decoding layers [5]. We also target the problem of automatic brain tumor segmentation on BRAT 2015 dataset. We particularly employed the UNET architecture for the propose task. In brats 2015, major challenges of brain tumors are irregular shape, size and localities; MRI Scans come with noise problem, and multiple modalities are needed to segment tumor sub regions. Therefore, we have employed a comprehensive U-NET architecture for segmentation.

1.2 Types of Brain Imaging Methods

X-ray, Ultrasonography, Computed Tomography (CT), Positron Emission Tomography (PET), Infrared thermography (IRT), Magnetic Resonance Spectroscopy (MRS), and Magnetic Resonance Imaging (MRI) are some of the new imaging technologies that have evolved in the last two decades [6]. The use of MRI to diagnose cancer of many forms, including glioblastoma brain tumors tissues, is becoming more common these days. A magnetic field and radio waves are used in the MRI procedure to provide a thorough pathology of the body.

MRI modalities are currently utilized to identify cancers in a variety of ways. A few of them are utilized to gain access to various parts of the brain. Each mode contributes to the provision of varied pathological information about tissues throughout the body.

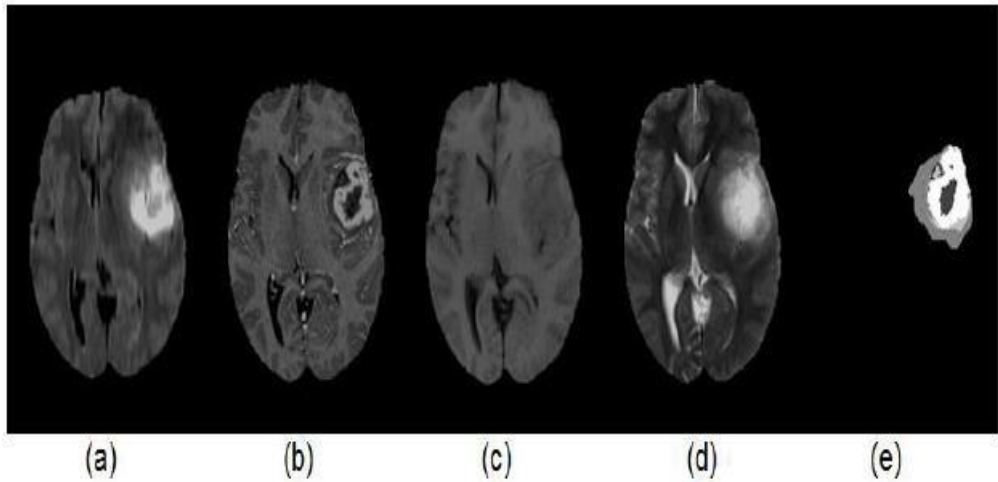


Figure 1.2 Scans of MRI T1 T1C T2 T2FLAIR and Ground Truth from left to right in BRATS 2015 Dataset.

1.3 Brain Tumor Segmentation and its Types

Glioma brain tumour segmentation can be done in three ways: manually, semi-automatically, and entirely automatically. Glioma tumour segmentation by hand is a tough and time-consuming task. The vast quantity of MRI pictures for a single patient must be evaluated by an expert. While in manual segmentation, pathologists use previous knowledge and experience to segment tumorous and healthy tissues.

Semi-automatic method requires both human and computer help to make segments. Manual and semi-automatic methods are very time-consuming and also the risk of human errors prevail.

On the other hand, Automatic-segmentation does not require human interaction. Computer algorithms draw the boundaries on the basis of knowledge which they have acquired during the learning process. This method does not take as much time as manual and semi-automatic methods take. The procedure is also devoid of human mistake. As a result, computer-assisted medical image analysis is a viable option.

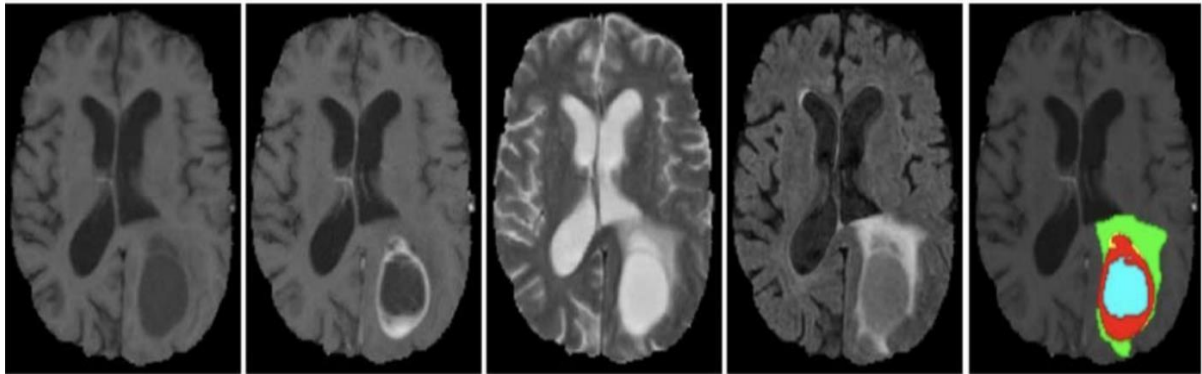


Figure 1.3 before and After Segmentation of Brain MRI images

Researchers have recently presented a number of autonomous image processing algorithms to segregate brain tumors tissues from healthy brain tissues. Because deep learning approaches produce the greatest results on huge datasets, they are included. Traditional image processing methods are also beneficial, but only for a limited collection of datasets, and they require the training of certain features. The process of recognizing a glioma brain tumors is extremely tough since two pixels with different labels may have the same attributes. This necessitates the use of a probabilistic machine learning algorithm that labels incoming images according to their likelihood. Among the several classifications, each image pixel is assigned to the one with the highest likelihood.

1.4 Research Challenge and Contribution

Because of the diversity in shape, size, and location of neoplasms, automatic glioma brain tumour segmentation is a difficult task. Furthermore, because these tumours lack obvious boundaries, segmenting them using typical edge-based approaches is difficult. The MRI pictures of glioma tumours derived from clinics and synthetic databases [9] are intrinsically complicated. Due to motion and field inhomogeneity, MRI systems emit noise during picture capture. These sounds could cause the intensity level of a picture to vary over time, resulting in poor segmentation performance. We used a variety of Convolutional Neural Network Architecture to solve the problem of glioma tumour segmentation. We played around with the U-NET architecture, which we somewhat tweaked. The U-NET architecture that results performs better at segmenting glioma tumours.

Throughout the architecture, a dropout layer has been inserted after every second convolution. We also swapped out the loss function optimizer and used the one that produced the best results for our problem.

1.5 Aims of the Thesis

The main objectives of this study include:

- An automatic glioma brain tumor segmentation framework is proposed having improved results.
- The proposed model uses complex Convolutional Neural Network Architecture to extract deep local and global contextual information from the data in order to segment different glioma tumor sub regions.
- Regularization, U-NET architecture, and Non-linear activations are used in the proposed model.
- We also used a two-phase network training strategy to address the issue of class imbalance, which resulted in improved performance.

1.6 Circumscription

Tissue images obtained from different sources may differ in appearance, something that will not be discussed in this study. In order to study dimensions of small histological images, magnification of the order of (40X) will be done and the size of the related image crops will be delimited. No research will be performed on the impact of contrast or color exploitation. Moreover, the results of CNN technique will not be compared with any earlier cancer grading findings since number of images used in different datasets are vary in prior research.

1.7 Structure of the Thesis

This research study has five chapters. Chapter 1 explain the challenges in Glioma Brain tumor Segmentation, Imaging Modalities, Segmentation methods, and Research Objectives A literature survey of the area of Glioma Brain Tumor Segmentation is offered in Chapter 2. We provided a detailed description of our suggested framework in Chapter 3. We reviewed the experimental setup and a few obstacles we met in Glioma Tumor Segmentation in Chapter 4. Chapter 5 contains a summary of our projected work as well as a discussion of feat.

Chapter 2: Related Background

2.1 Tumor

Normally, the cells in a human body grow and divide in an order. Every cell in a body performs a certain job and when old cells are destroyed, new cells take their place and the cycle goes on. But when cells divide in an uncontrolled way and do not die, they form an unnecessary mass of tissue called tumor. The tumor keeps on growing if more and more cells continue to accumulate in the mass. While some tumors are benign, others are malignant.

2.2 Brain Tumors Scans

Based on the extent of human involvement, segmentation of brain MRI images approaches are divided into three categories (manual, semi-automated, and fully automatic). All of these methods for treating brain tumours are currently in use, with varying degrees of success.

With a prior understanding of human brain architecture, radiologists use information gained from several multimodal scans of a single patient in manual segmentation [11]. Radiologists achieve this by manually drawing the boundaries of a brain tumour and color-coding the various tumour locations. Because an expert must examine each slice of the patient's MRI, this is a time-consuming task. Furthermore, the expertise and attention of the expert matters a great deal in terms of performance. As a result, semi-automated and completely automatic procedures are increasingly employed in conjunction with manual approaches to achieve superior results.

In semi-automatic approaches, the user initiates the process by entering some parameters, then waits for the results and responds to the software computation. Initialization, feedback response, and evaluation are all part of this process [12].

This process may result in better performance but it also depends upon the expert and may vary for some experts on repetition.

Based on a region expanding segmentation tool, Thomas [13] suggested a method for semi-automated tumour segmentation. Using a smart brush tool, 320 segments of Flair and MPRage sequences were segmented (a region growing based semi-automated tool). The algorithm begins with a segmentation-aiding region-growing algorithm, followed by a 2-D segmentation that was manually conducted and then 3-D interpolated after conducting another perpendicular 2-D segmentation. Small alterations were also done manually or with the help of the region expanding tool. The proposed methodology performed well, but the existence of manual help in the methodology caused performance to vary for each individual.

The majority of research nowadays is conducted using a fully automated segmentation technique. It doesn't require any user participation and takes a fraction of the time. This is one of the most difficult segmentation tasks because to the irregular shape, variable size, and location of tumours. We classified fully automatic approaches into four categories:

Neural Network methods, traditional image processing methods, clustering methods, and traditional machine learning methods are all examples of traditional machine learning methods.

2.3 Conventional Image Processing Approaches

Most traditional image processing algorithms concentrate on the geometry of a picture. The value of pixels in an output image is determined by the surrounding pixels of the matching pixel in the input image. The region expansion method is the most extensively used morphological operation algorithm. It is used to extract relevant pixels from a snapshot in a similar region. In calculating the similarity criterion, the range of pixel intensity levels is the most essential consideration. However, the partial volume impact is a drawback of the region-based strategy. Because the voxel represents more than one tissue type, it appears on that pixel, which is actually the border of two tissue types, causing the pixel to blur.

Sudharani et al. [14] proposed a morphological method for segmenting brain tumours. In this technique, the brightness modification strategy was utilized first, followed by the resampling of a photograph. They then utilized a histogram normalization approach to transform the grey photographs into vibrant images. The tumour area was then computed using geometrical procedures, and the region of interest was highlighted using a threshold methodology. Before applying erosion and dilation, the fast Fourier transform and lookup table conversion were used. The accuracy of their system was 89.2 percent. Ishmam et al. [15] suggested an approach in which a dynamic threshold was used to identify a region of interest, and then k-mean clustering was used to segregate tumour regions. Following that, a high-intensity region-growing approach was used. 12 as a tolerance value. On the brats 2012 data set, the proposed technique has an efficiency of 0.85. The approach was also capable of accurately calculating the size of the tumours.

The BRATS 2012 dataset features a small number of photos, as has been highlighted. It means that they are inefficient when it comes to deep learning algorithms, which require a larger dataset to be effective. As a result, traditional image processing-based methods perform well with smaller datasets. Traditional image processing has a substantial advantage over deep neural networks in this regard.

2.4 Primary Machine Learning Algorithm

Medical image analysis and diagnosis can be automated using traditional machine learning algorithms. Random Forests and Support Vector Machine are two of the most commonly used technologies, and they have the potential to considerably reduce the workload of radiologists in the area of radiology. Random Forest is a versatile, user-friendly algorithm that gives excellent classification results in the vast majority of scenarios. They are the most widely used algorithms due

to their simplicity and adaptability in terms of classification and regression Random forest RF is a supervised learning approach for constructing random forests, which are a collection of decision trees that have been bagged trained. Nicholas et al. [16] proposed a supervised learning technique based on random forests-derived probabilities, in which they used multiple sets of features such as intensity, shape, and asymmetry to segment total brain and tumour regions. By creating a matrix of attributes with their labels, they employed a random forest training technique to predict the label. Each image sample passes through the ensemble's trees, where it is classified and labelled. Each vote was converted into voxel-wise probabilities estimates for each class using some method. They employed two stages of RF training to complete the brain tumour segmentation challenge.

A new segmentation method based on super pixel classification and segmentation was proposed by Mohammad reza et al. [17]. They extracted a number of different properties from each super pixel of the Flair MRI scans.

In order to compare their outcomes, they also trained these features on the support vector machine (SVM).

When given labelled input training data, a support vector machine produces an ideal hyper plane that can categories each new test case.

Vladimir Vapnik devised first support vector machine. a highly valuable real-time technique that requires minimal computer power while maintaining great accuracy. Such algorithms can be highly useful in medical imaging where high processing power is difficult to get by and time is crucial. A random forest and SVM-based technique was developed by Samya et al. [18]. Their strategy began with the use of RF to categories foreground input pixels and generate segmentation results, which were then passed on to the SVM classifier. The SVM classifier then segmented a large region of interest (ROI) that had been absent during the initial stage. As a result, SVM concentrated on global characteristics while RF concentrated on more local characteristics. These two processes were carried out again and again until the best results were achieved.

2.5 Clustering Techniques

Clustering is an unsupervised machine learning approach that requires no prior knowledge of pixel labels. In supervised machine learning algorithms, each sample consists of two parts: an input characteristic and a label. The purpose of supervised learning is to create a functional relationship between training and testing data. Unsupervised learning techniques come in handy when pixel labels aren't provided. In terms of execution time, the clustering technique has an advantage over the deep neural network because these techniques are much faster. Table 2.1 lists the benefits and drawbacks of various techniques.

Table 2. 1 Advantages and disadvantage of various image processing method.

| No. | Method | Advantage | Disadvantage |
|-----|---------------|---|--|
| 1 | Clustering | For small data sets, clustering is a quick and simple procedure. When compared to deep neural networks, clustering algorithms are substantially faster to implement. | In comparison to Deep Convolutional Neural Network techniques, performance is significantly lower. |
| 2 | SVM | SVM is a very valuable real-time method since it utilizes very little computer resources while providing great accuracy. Also, even if the training data isn't particularly large, the SVM method can perform well. Small changes in data will not alter the results once the limits have been determined, avoiding over fitting. | When compared to Deep Neural Network Methods, performance is much lower. |
| 3 | Random Forest | Random forests are a straightforward method that may be used for classification as well as regression. Like SVM method, random forests reduce variance and helps is avoiding over fitting, | Feed forward neural networks are unable to learn nonlinear low-level representations. Another downside of the random forest technique is that it performs poorly on data with uneven classes. (An unbalanced class problem exists in the BRATS dataset.) |

| | | | |
|---|---------------------------------------|--|---|
| | | | |
| 4 | Conventional Image Processing Methods | Geometrical procedures, for example, require extremely little training data. It takes less time to classify the data. | When compared to the Deep Neural Network DNN technique, the performance is lower. |
| 5 | DNN | While most classification algorithms require meaningful features as input, DNN may be able to discover meaningful features from training data on its own. Methods of deep learning In numerous areas, it outperforms other classification problems by a large margin.. | |

For the detection of brain cancers, many systems employ k-mean clustering. Although K-mean clustering is a rapid and easy way to deal with large data sets, it can sometimes lead to partial tumour detection, which can be costly if the tumour is malignant. In K-mean clustering, each data point must belong to just one cluster center. Other systems, on the other hand, use fuzzy C-mean FCM clustering, which does an excellent job of segmenting all tumour regions..

In fuzzy C-mean clustering, a point must belong to at least one or two cluster centres. The k-mean integrated with fuzzy C-mean clustering (KIFCM) methodology, which is a hybrid clustering method, was proposed by Eman et al. [19]. Before sending the input photographs into the KIFCM algorithm, they first de-noised them. The KIFCM was used to segregate the tumour from the surrounding healthy tissue. It helped segment and categories more dispersed points into one or more kinds. The DICOM dataset, the Brain Web data collection, and the Brats data set are used to evaluate their findings.

James et al introduced another method based on Otsu and fuzzy C-mean clustering, who used the VelocityAI programmer to build tumor zone of interests blobs for Otsu and Fuzzy processing. These blobs were then used to segment the tumours using clustering algorithms. With three and four classes, the Otsu and Fuzzy C-mean clustering algorithms were applied respectively. With a dice score of 0.91, their Fuzzy3 (three classes) method was the most successful. Table 1 compares the various image processing approaches used to segment glioma tumours.

2.6 Convolution Neural Networks Approaches

The most widely used brain tumour classification algorithms are neural networks, which are particularly popular among academics due to their better performance. The input layer, convolution layer, pooling layer, drop-out layer, fully connected layer, and final output layer are all layers found in popular neural networks. The most often used deep neural network approach for image identification and segmentation is convolutional neural networks. While most classification algorithms require meaningful input, CNN can automatically learn meaningful features from training data.

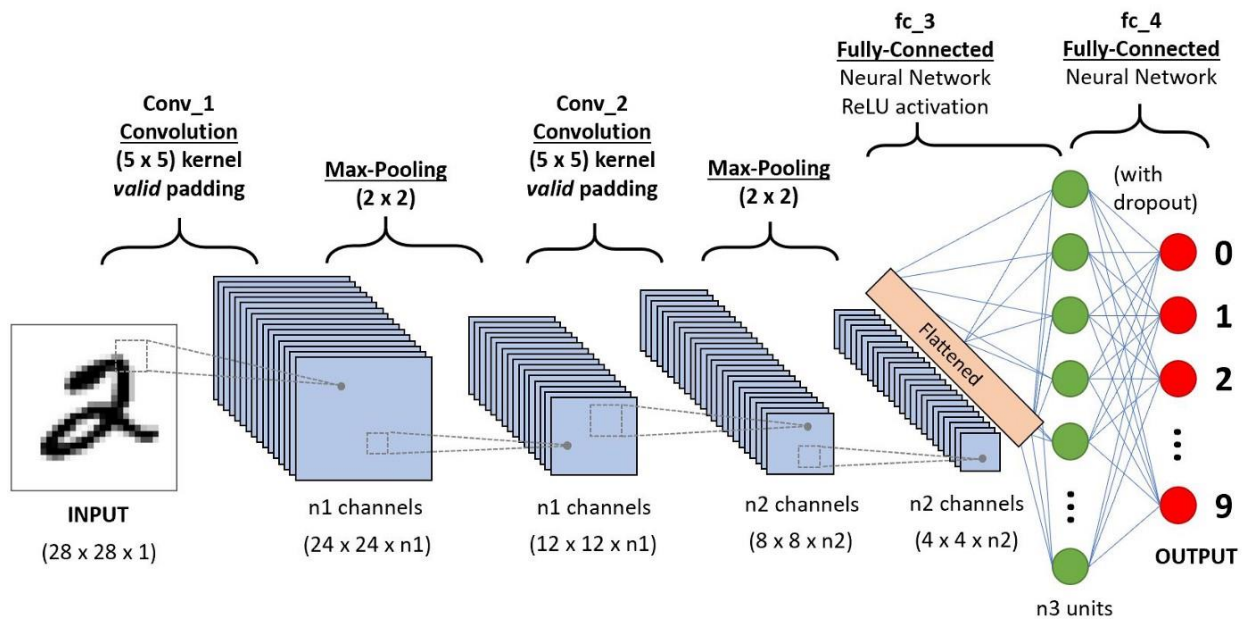


Figure 2.1 CNN Basic frameworks

Small leakage patches were convolved using a sequence of 3×3 kernels, then a max-out and max-pooling layer was added, according to Mohammad et al. [22]. The max-out layer compares the input feature values for each spatial point and provides the maximum value of a feature map. They also used a two-pathway architecture, which has two streams of input patches, one with a small 7×7 (local) receptive field and the other with a big 13×13 (global). Both methodologies provide different feature maps, which were integrated to create a single feature map with both local and global receptive field features. On the Brats dataset, their methods achieved a dice score of 0.85.

Saddam et al. [23] proposed a nexus architecture in which two CNNs were used with the output of the first network concatenated with the input of the second. They demonstrated a variety of nexus architecture principles. The BRATS dataset provided a 33×33 input patch. To refine the design even more, they used the dropout and batch normalization layers. As a pre-processing step, they used N4ITK and the intensity normalization technique. On the Brats 2015 dataset, these sophisticated nexus designs were able to earn good dice scores.

The majority of brain segmentation algorithms are two-dimensional, but Konstantin et al. [24] developed a 13-layer deep three-dimensional brain tumour segmentation architecture. For a more detailed feature field, they used a smaller kernel in their design. Furthermore, they obtain both local and contextual data using concurrent multistate processing. They achieved this by combining the inputs of two routes into one, but the second segment, which had similar low resolution, was down sampled by a factor of three. On the dice, their architecture obtained a score of 0.90.

The purpose of this architecture was to extract as many local and global features as possible. Five pieces were cut out of their network. Both input and output were included in the first slice. On the right side of each slide, the de-convolution process was carried out. The reset50 architecture was used on the left side of each slide, from top to bottom. Each ResNet50 was connected to a DCR, and the results were combined with lower layer's DE convolution process to create a complicated architecture. On the dice score, their proposed method worked admirably.

As a pre-processing step, Sergio et al. [26] used N4ITK and the intensity normalization approach.

They also included a post-processing step that deleted small groups that were smaller than the threshold level. In the BRATS 2013 competition, their algorithm came in second place. The majority of brain tumour algorithms have been discovered to lack a post-processing technique, which could help improve the system's performance. As a result, a researcher should place a strong emphasis on the algorithm's post-processing. Table 3 compares the results of the top Glioma tumor segmentation technique.

2.7 Dataset

Various organizations have various datasets to motivate researchers to take active participation in brain segmentation. Among these multiple datasets some are listed below i.e. ISBR (provided by Massachusetts General Hospital), DICOM (online accessible dataset with images and videos), and BRATS that are publicly available [12, 13]. The datasets mentioned below are used to conduct the majority of automated brain tumor segmentation methods since they allow for reproducibility and comparison of findings across studies.

Various committees have offered various datasets to encourage researchers to participate in brain segmentation. Brain Web [27], Internet Brain Segmentation Repository (ISBR) [28], and BRATS [29] for tumour segmentation, Isles [30] for evaluating stroke, MSSEG [31] for lesion segmentation and detection on MS data, and NeoBrainS12 [32], MRBrainS [33] are some of the most widely used publically available datasets. The datasets described below are used to run the majority of automatic brain tumour segmentation algorithms because they allow for replication and comparison of results across research.

2.7.1 DICOM

DICOM (Digital Imaging and Communications in Medicine) is the world's largest online collection of medical images and video data. It is one of the most extensively utilised platforms for free and open datasets. It has a big database of medical data for a range of illnesses, including glioma brain

tumours. Optical Coherence Tomography, Mammography, and Magnetic Resonance Imaging images are included.

Various performance measuring matrices are used to analyze and compare the accuracy of a model. Multiple metrics are utilized to evaluate performance in various procedures, including true positive, true negative, false positive, and false negative. Table 1 displays a collection of different performance measurement methods for evaluating the quality of brain MRI segmentation, as well as their mathematical formulation.

2.7.2 ISBR

It's an MR Images dataset from Massachusetts General Hospital's Center for Morphometric Analysis. IBSR18 and IBSR20 are the two sets of data that make up this dataset. IBSR18: This dataset is made up of T1-w scans with a 1.5mm slice thickness. It is free of any noise that could compromise scan accuracy. Auto bias field correction was used to preprocess the data.

2.7.3 BRATS

In 2012, the Multimodal Brain Tumor Image Segmentation Benchmark (BRATS) competition was established to evaluate and compare several brain tumour segmentation techniques. It consists of a large number of MRI images of brain tumours that have been separated into five categories: healthy tissue, edema, non-enhanced, necrosis, and enhanced tumour regions. Over time, the training dataset has grown in size. There are both low-grade and high-grade samples in the sample. t1 mri, t1 contrast-enhanced mri (t1c), t2, mri and t2 flair mri are the four imaging modalities available. The voxel resolution of all images in the Brats datasets is 1 mm. The BRATS dataset serves as a reference point for comparing outcomes from different studies.

Figure 2.2 depicts a detailed modification.

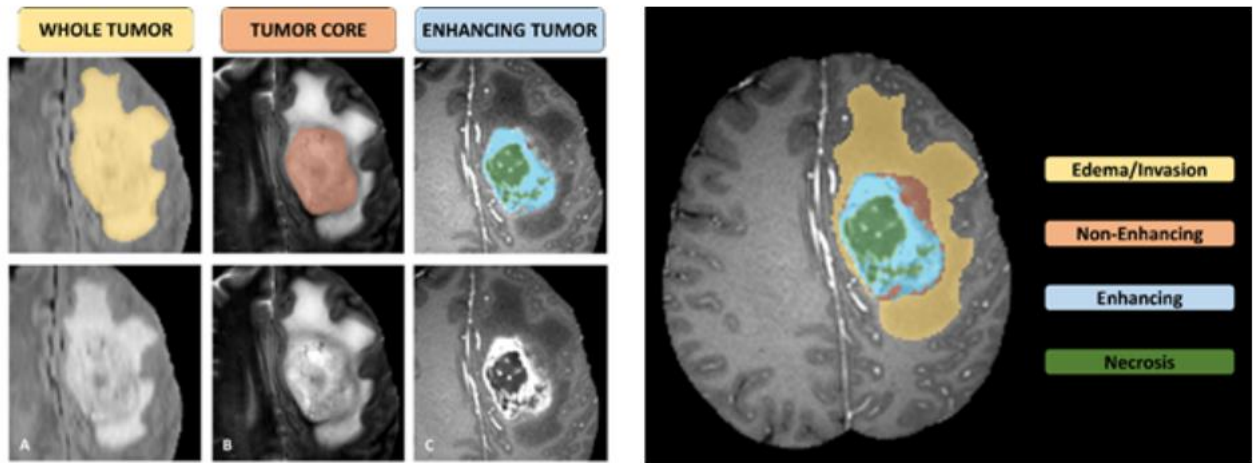


Figure 2.2 Sub region of Glioma

The BRATS dataset was introduced in 2012 with MRI scans consisting four different modalities. Segmentations and classifications approaches applied on BRATS challenges which produced satisfactory results. Dataset consisted of five major classes named as healthy brain's cells, non-enhancing brain tumor, edema, enhancing tissues of tumors and lastly necrosis. With every year, training size of dataset has been growing continuously. There are two types of tumor grades in dataset. One is low grade and other is high grade tumor. The BRATS dataset contains MRI scans with different modalities named as T1, T1 contrast-enhanced (T1C), T2 and T2 FLAIR. The dataset serves as a benchmark for analyzing the outcomes of different brain tumor segmentation techniques.

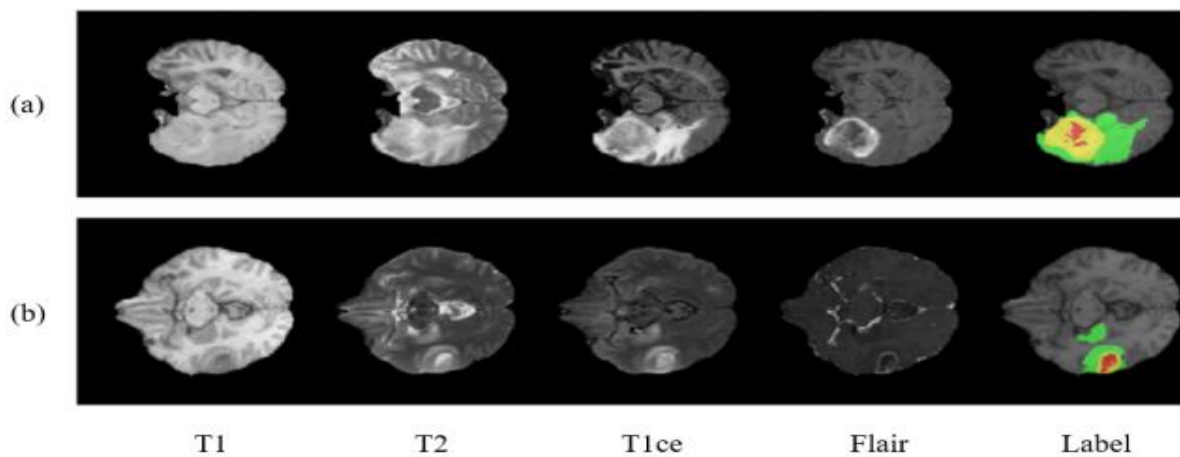


Fig. 2.3 First four MRI scans are four MRI modalities and on the extreme right corner there is a ground truth.

2.8 Challenges and Problems

Automatic glioma brain tumour segmentation is difficult due to the diversity in shape, size, and location of these neoplasms. Traditional edge-based techniques are difficult to segment because these tumours have uncertain boundaries with discontinuities. MRI pictures of glioma tumours from clinics and synthetic datasets are intrinsically complicated.

Chapter 3: Methodology

In this chapter, we'll go through the extensive feature engineering-based models that are used to segment brain tumor manually. Then, using convolutional neural networks, some recent deep learning-based models for segmentation and pixel level classification were presented (CNN). Finally, we review the Pixel level classification using UNET architecture upon which our proposed method is based.

3.1 Overview of overall Proposed Methodology

The subject of gliomas brain tumors segmentation was the focus of our proposed research, which used the modified U_NET architecture. Images were taken from the BRATS 2015 dataset. Pre-processing, patch construction, and implementation of various CNN architectures are the three steps in the proposed methodology. The input images are first preprocessed and divided into patches, which are then fed through the proposed architecture. The flowchart of our suggested framework is shown in Figure 2. The following is a more extensive description of these steps. Our proposed paradigm is depicted in Figure 3.1 as a block diagram.

There are three segmentation techniques that are highly depended on human's interaction level. These techniques are named as manual, semi-automatic and fully automatic.[14] Among these segmentation methods, manual segmentation uses prior information of the single patient with definite amount of human brain knowledge through past training and experience [15].In this section, we first discuss U-NET architecture along with Relu activation function for segmentation of brain tumor on BRATS-2015 dataset. Then, proposed a Mask-RCNN for classification of brain tumor which resultantly gives better performance. Figure 3 shows the complete procedure of our designed methodology.

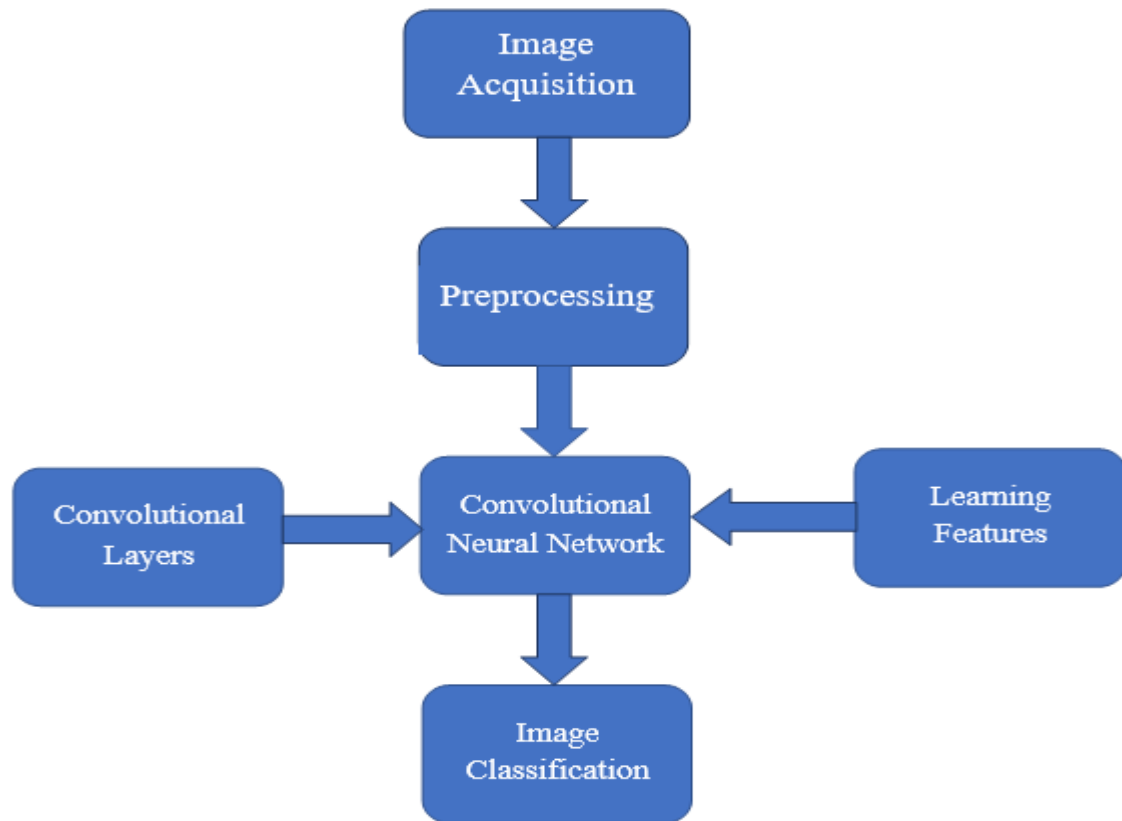


Figure 3.1 Proposed Approach of training and testing algorithm

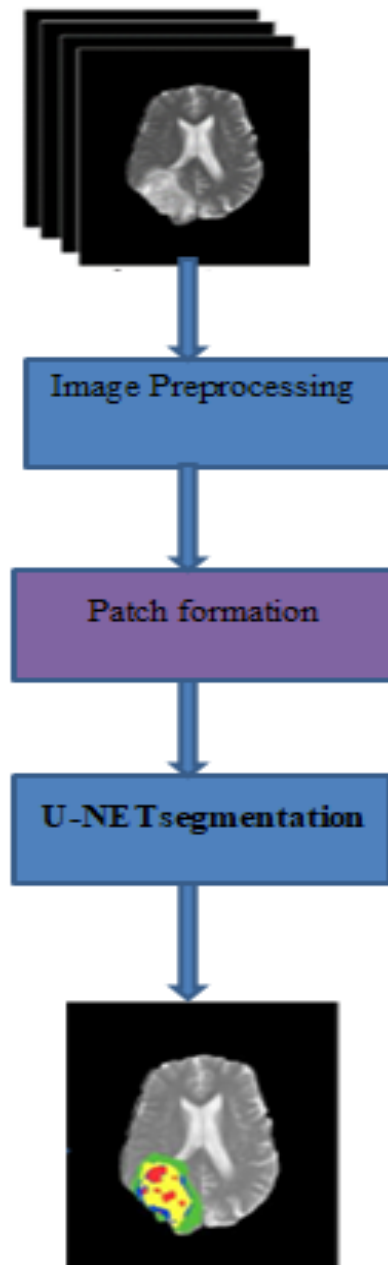


Fig. 3.2 Block diagram of our proposed model

3.2 Image Preprocessing

MRI images have noise problems because of heterogeneity and motion of images throughout image acquisition. These noises can cause an image's intensity level to change and consequently resulting in poor output. Two pre-processing techniques are applied to enhance our input images. Firstly, all images are homogeny using the N4ITK algorithm, which is a bias correction technique. The N41TK algorithm is capable of correcting MRI data's bias region. Secondly, the intensities in

the top 1% and bottom 1% are ignored. Secondly, each picture in our dataset was also subjected to intensity normalization. This process of normalization translates the image's pixel intensities into a functional collection. In this process we removed 1% top and bottom intensity values throughout the dataset which helps improving the learning process during training. To improve our input photos, we use two pre-processing approaches.

1. To eliminate this effect, N4ITK [37], a bias field correction approach, is applied to the input images. N4ITK eliminates inhomogeneity un the input data created during MRI scan capture. Normalization of non-parametric, non-uniform intensity also the N3 technique is a well-known approach for removing artifact-induced intensity normalization. N4ITK is a better variant of N3ITK.
2. Each image in our dataset was also subjected to intensity normalization. The intensity normalization method converts pixel intensities across the image into a usable range. We deleted 1% top and bottom intensity values throughout the dataset as part of this process, which aids in the learning process during training.

The impact of pre-processing techniques such as N4ITK and normalization is depicted in the diagram below. On the BRATS 2015 dataset, Figure 3.2 compares the MRI image before and after applying pre-processing.

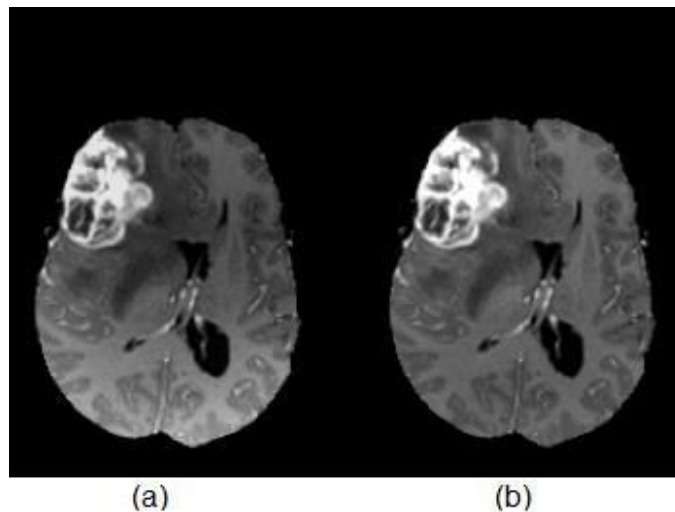


Figure 3.3 after image preprocessing results

3.3 Formation of patches

The BRATS-2015 dataset consists of 3-D MRI images along with T1, T1c, T2, and FLAIR modalities. All these 3-D brain images are transformed into 2-D MRI slices having pixel size of 240 x 240. Further, patches are generated from these multiple slices and modified U-NET is trained on them. We tested on different size of patches to see which patch size give better results. After experimentation we choose patch size to be 33X33 throughout the dataset. The label of the center pixel of each patch is assigned as a label to that whole patch. Similarly, same step is repeated throughout the dataset.

3.4 U-NET framework for brain tumor segmentation

In our proposed work we address the problem of gliomas segmentation in brain images using U-NET architecture. We acquired images from BRATS 2015 dataset. The proposed methodology is divided into three main steps named as image preprocessing, patch formation and U-NET architecture. These steps are described briefly following.

3.4.1 U-net architectural detail

To the best of our knowledge the U-NET architecture has not been realized on the BRATS-2015 dataset. Figure 4 shows the overall proposed U-net architecture which include encoding and decoding blocks. The Architecture below takes images of size 33×33 and generates output of the same size after implementation. The left side of the architecture acts as an encoder and the right side of the architecture acts as a decoder. In convolution layers activation functions such as soft_max and relu. Further, padding is used to get same sized output images.

3.4.2 Generic U-NET architecture

- First sight, it has a “U” shape. The architecture contains two paths. First path is the contraction path (also called as the encoder) which is used to capture the context in the image.
- The second path is the symmetric expanding path (also called as the decoder) which is used to enable precise localization using transposed convolutions. It is an end-to-end fully convolutional network (FCN), i.e. it only contains Convolutional layers.

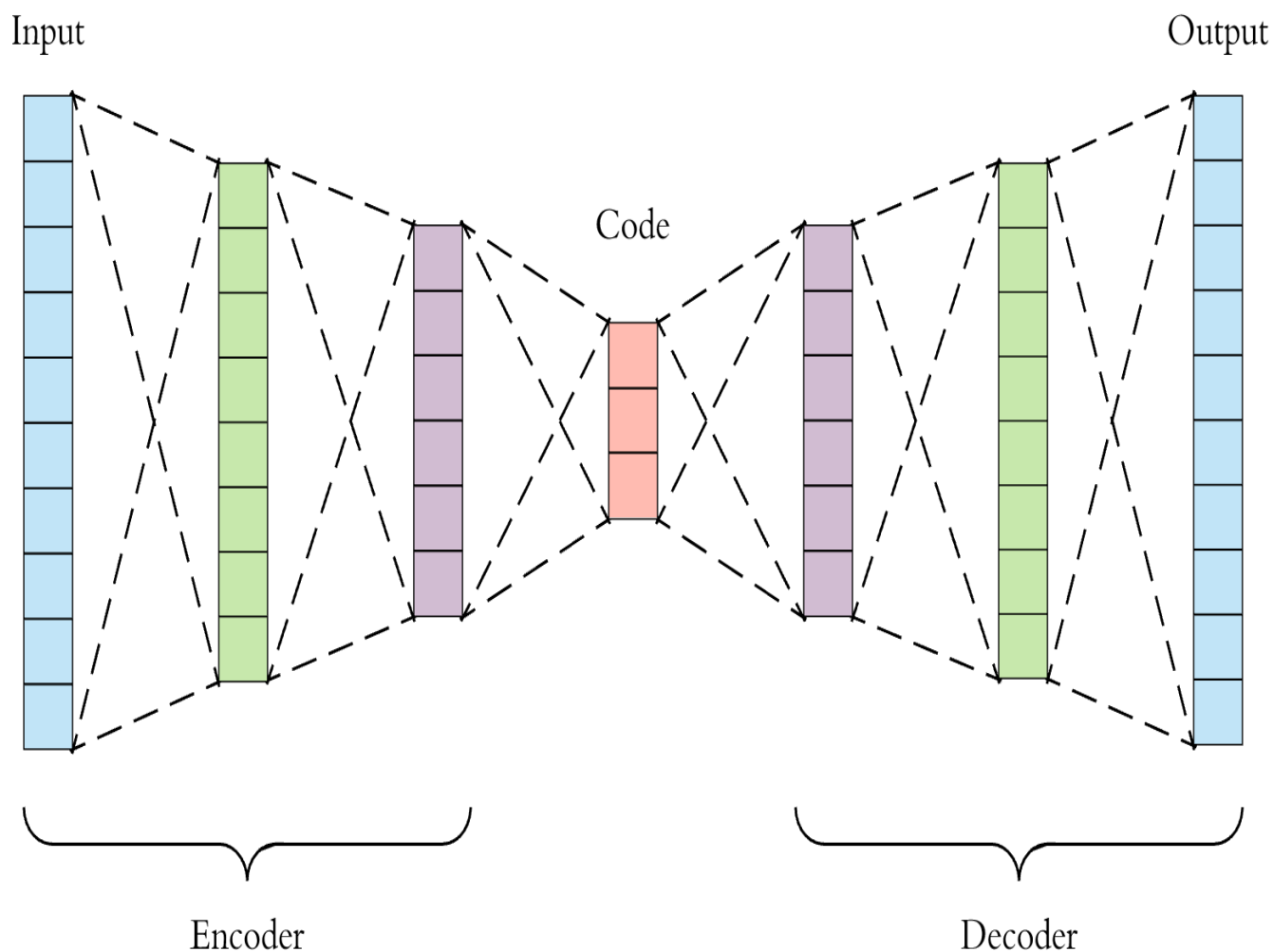


Figure 3.4 Generic U-NET Architecture

3.5 Modified U-NET architecture

The proposed Architecture below takes images of size 33×33 and generates output of the same size after implementation. The layers of a convolutional neural network (CNN) are convolution, pooling, activation, dense, batch normalization, and dropout. Each of these layers has its own set of functions. A feature map is created by layering these layers on top of each other in a hierarchical order. Each layer receives features from the previous layer and passes them on to the next layer. The most significant layer in a CNN is the convolutional layer, which is made up of the building blocks of a Convolutional Neural Network. The feature maps produced by the convolution layer and convolution filter are transferred to the pooling layer. The pooling layer keeps the features that are valuable and discards the rest. These maps move through each layer of the network until they reach the last layer, which is usually the final layer of the network. Our suggested modified architecture is depicted in detail in Figure 3.5. The figure shows that two pooling layers are used, the first of

which is max pooling and the second of which is average pooling. In our suggested modified U-NET architecture, we've included a dropout layer after each convolution layer. Each module now produces better output and has more regularity as a result of this addition. Many architectures employ a dropout layer to prevent over fitting. Some researchers utilize dropout as a replacement for batch normalization, but a few studies [45] claim that Dropout works equally well as batch normalization in terms of generalizing the result.

Convolutional filters are combined with a Convolution layer to create feature maps. These filters are available in three different sizes: 3x3, 5x5, and 7x7. Convolution filters (also known as kernels) are often little box-shaped objects that look like the objects in the photos. The resulting feature, termed feature maps, contains essential information in the form of little boxes. Each feature map corresponds to a hidden unit known as a neuron, which is controlled by the activation layer.

Convolutional Neural Networks use a variety of activation layers, including Sigmoid, Tanh, ReLU, leaky ReLU, and max-out [43]. The surrounding voxels in the feature map are affected by the activation. Neuronal receptive fields are the areas in the feature map that grow in size with each succeeding layer. Each neuron in a layer is connected to the layer above it via a weighted link.

T1, T1c, T2, and Flair are the four patches that the proposed framework processes. These four patches are combined into a single input that is sent to the network. The network considers the input to be a single four-channel input. One modality is represented by each channel. These phenomena are comparable to those seen in color images' red, green, and blue channels. The procedure continues, with each slice of the entire brain being thrown out.

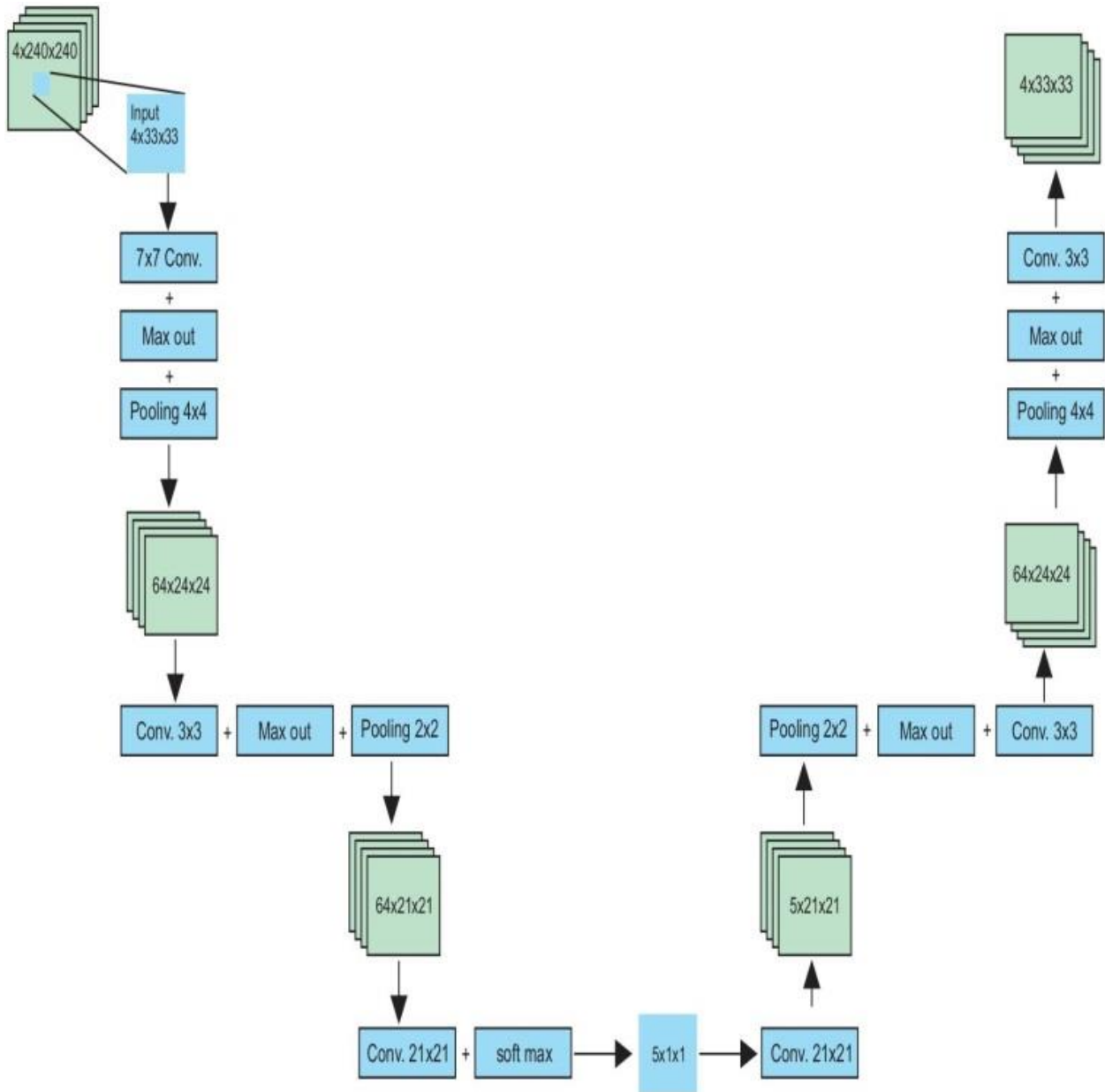


Figure 3.5 Proposed Modified Tuned U-NET Architecture

3.5.1 Encoding side: left side of the architecture

There are few sections of encoding framework of architecture. Each section comprises of convolution layer, a max-out and a pooling layer. For example in figure 4 input image of size four patches of 240×240 are indulged and extract four patches of 33×33 as a input. On this section 7×7 convolution filter is applied with couple of max-out activation function and a 4×4 pooling function. In the same way all the layers are working as described in the diagram. The last section of the encoder side is used activation function soft-max and output is $5 \times 1 \times 1$ as final output on the encoder side of the architecture. Conclusively, it can be said that on the encode side of the

architecture process of contraction is applied for better features learning. Further, details of all the layers is on the table 1.

TABLE 3.1: DETAIL OF ALL THE ENCODING LAYERS

| Encoding Layers | | |
|-----------------|----------------------------|-------------|
| Layers | Layer detail | Output Size |
| Conv1_x | 7×7, Pooling 4×4,Maxout | 64×24×24 |
| Conv2_x | 3×3, Pooling 2×2,Maxout | 64×21×21 |
| Conv3_x | 21×21, Soft- max | 5×1×1 |

The encoder network performs convolution with a filter to produce a set of feature maps

- ReLU is applied
- Batch normalized
- Maxpooling with a 2×2 window and stride 2 is performed
- Discard FC layer

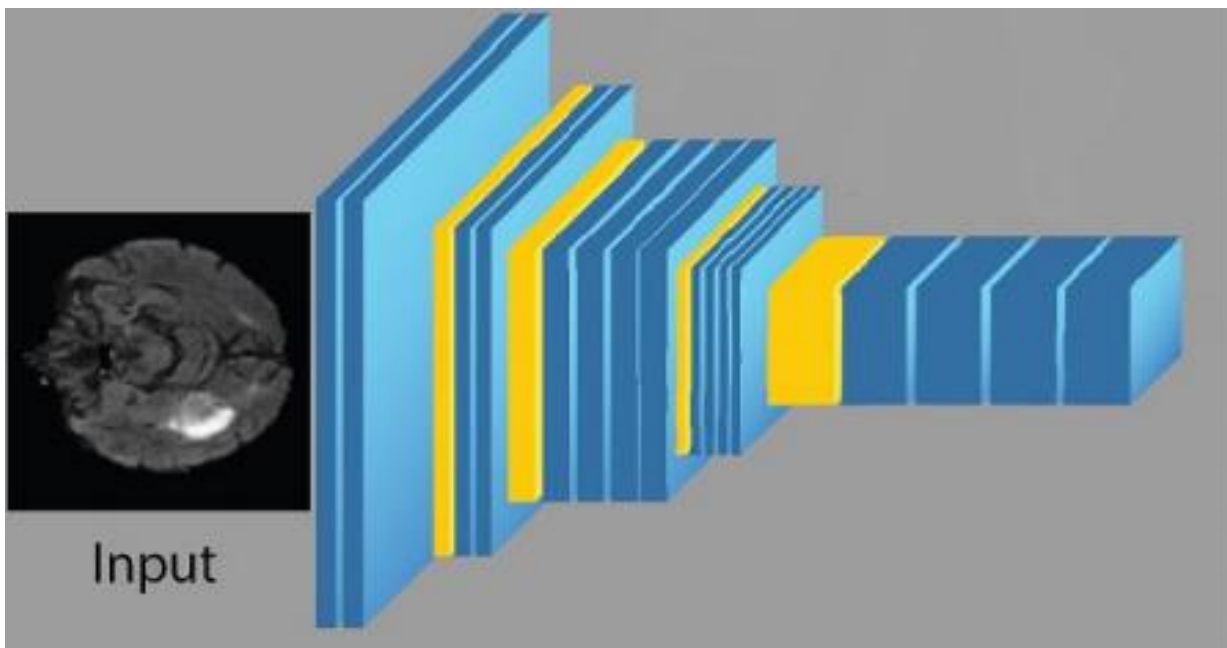


Figure 3.6 Encoding working side

3.5.2 Decoding side of the architecture: right side

The right side of the architecture named as decoder side performs the expansion process. In this portion all the decoding layers work in a reverse order as compared to encoding layers. All the convolution layers show in table 2 of U-Net are followed by pooling layer and soft-max activation function. Further, detail is given below;

- The decoder network up samples its input feature map.
- Batch normalization is applied.
- The decoder corresponding to the first encoder (front to the input image) produces a multi-channel feature map.
- The high dimensional feature representation at the output of the final decoder is fed to a trainable Soft-max classifier.
- The output of the Soft-max classifier is a K channel image of probabilities.

TABLE 3.2: DETAIL OF ALL THE DECODING LAYERS

| Decoding Layers | | |
|-----------------|-------------------------------|-------------|
| Layers | Layer detail | Output Size |
| Conv1_x | Convolution 21×21 | 64×21×21 |
| Conv2_x | 3×3, Pooling2×2,Max out | 64×24×24 |
| Conv3_x | 3×3, Soft_max | 4×33×33 |

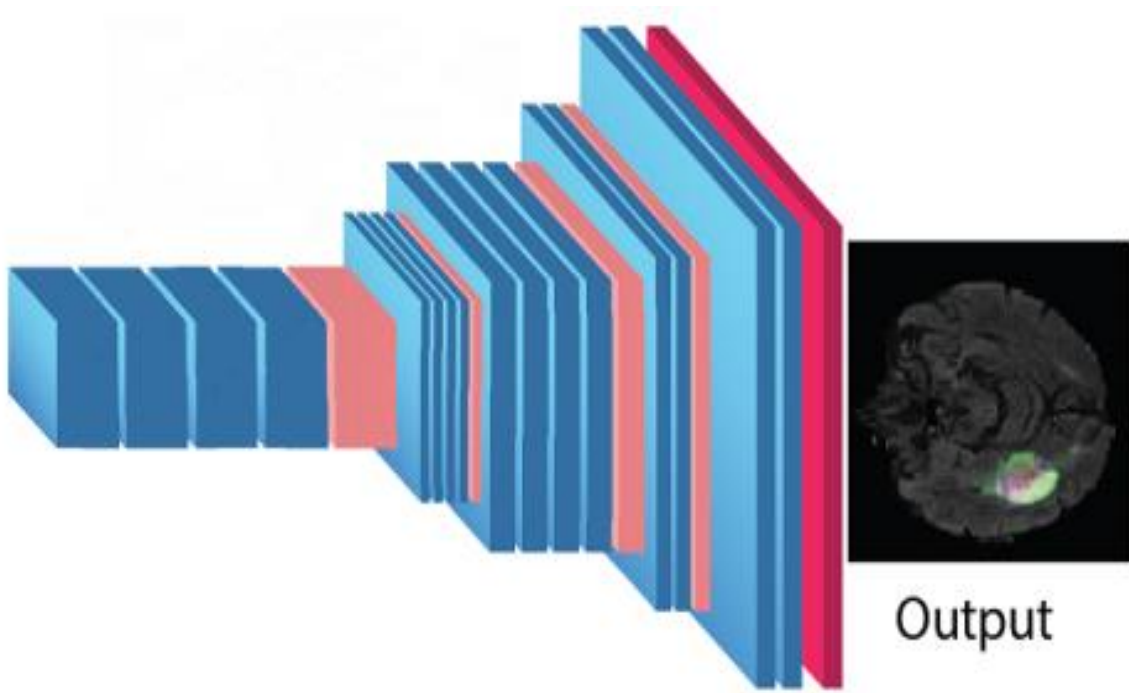


Figure 3.7 Decoding working side

3.6 Training

To enhance the proper training probabilities of labels across the dataset while reducing the loss function, Convolutional Neural Network training is necessary. The objective is to optimize the Softmax layer probability for each training patch's true label across the whole dataset. On the network, various loss function optimizers were evaluated in order to maximize training performance and reducing. Figure 3.5 depicts a random selection of kernels at various points in the proposed modified U-NET architectures.



Figure 3.8 Training Kernel size

3.6.1 Loss Function

The loss function is an important component of both neural networks and convolutional neural networks. They're described as a metric against which the network's performance is measured. In our study, we used the mean square loss function because we needed pixel-by-pixel data.

3.6.1 Optimization of loss function

To fine-tune our outcome, we trained the network using three loss function optimizers.

- We started using stochastic gradient descent (SGD), which is commonly regarded as the default optimizer. Then we used Adam optimizer to further test our network.
- Finally, the influence of Root Mean Square Propagation (RMSProp) optimizers on finding the global minimum point of the loss function was investigated.

3.6.2 Batch Normalization

- Sometimes layers weights change significantly due to large learning rate, causing small changes to amplify resulting the weights to explode.
- Batch normalization control the gradient in acceptable range.
- It maintains the feature's mean and standard deviation close to 0 and 1 respectively.

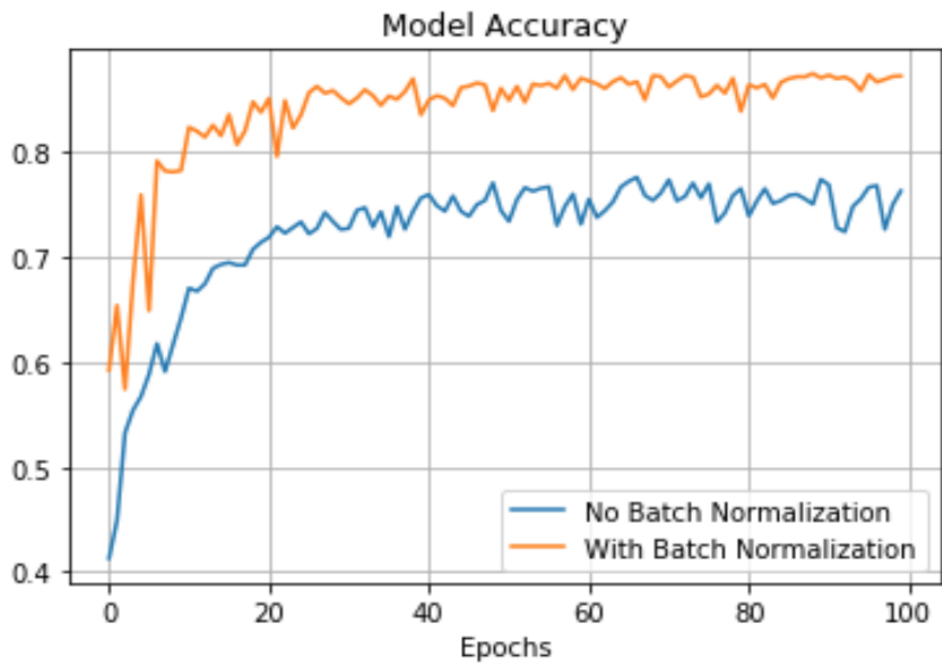
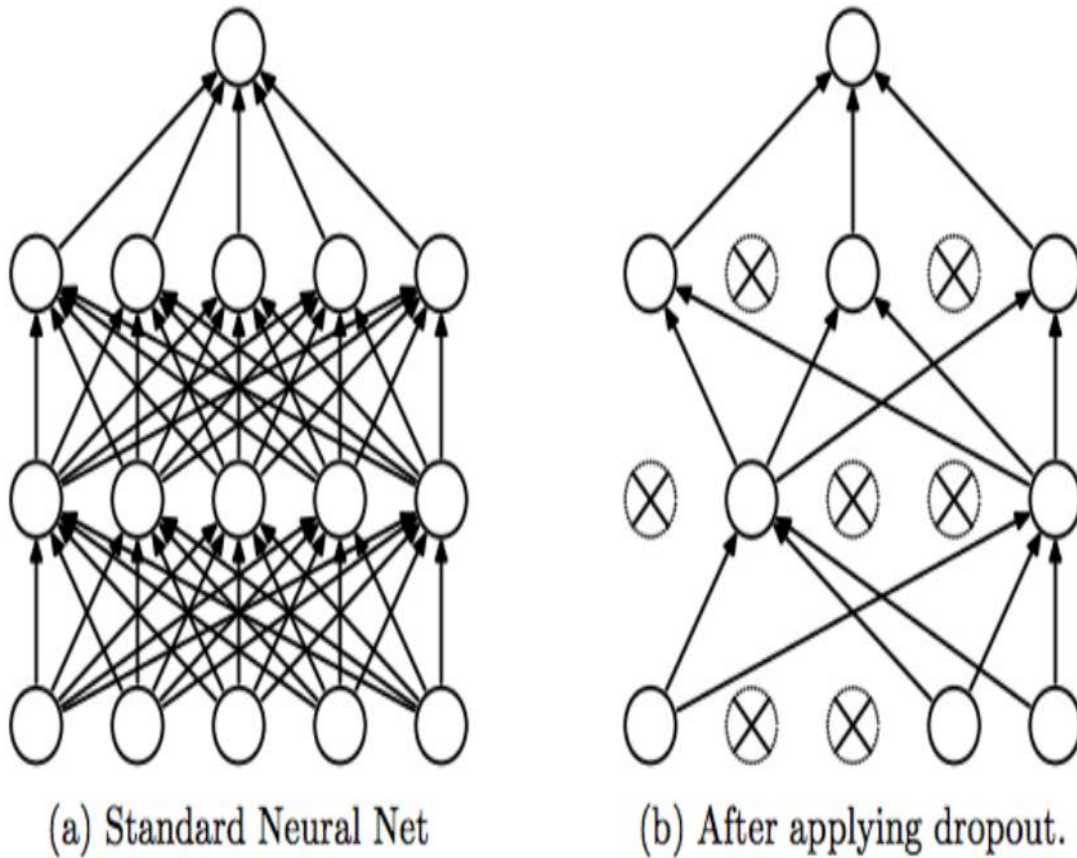


Figure 3.9 Batch Normalization

3.6.3 Dropout Layers

- Large neural nets trained on relatively small datasets can overfit the training data.
- Results in poor performance when the model is evaluated on new data.
- Technique to avoid over-fitting.
- Drop random set of Neurons from each layer.
- Reduces computational complexity.
- Dropout value is set at 0.3.



3.7 Implementation: Hardware detail

- Architecture was trained using Core-i9 9th Gen. Linux mint machine with RTX 2080 11 GB graphics card and 64 GB RAM and 1TB SSD.
- The primary language used was Python.
- NumPy and SciPy were used for the vast majority of numerical computations.
- Scikit learn was used for the machine learning algorithms.
- All deep learning related code was written using Keras, with a backend of Tensor Flow.

3.8 Network Training

- Four images of 33*33 pixel are passed through the network as input.
- We trained the model till the convergence was achieved.
- We used max and average pooling layer in our model
- Dropout value of 0.3 is adjusted to drop weak feature in the training.
- The network was trained by using batch training method with batch size equal to 64.
- We set the biases value of all layer to be zero except for the last soft-max layer where we set the bias value to be 0.2.

Chapter 4: Experimental Results

4.1 Dataset description

Our experiments were conducted using the BRATS 2015 [29] dataset, which serves as a benchmark for evaluating brain gliomas tumors segmentation. The training dataset contains 220 HGG and 54 LGG patients' MRI scans, whereas the test dataset contains 110 images.

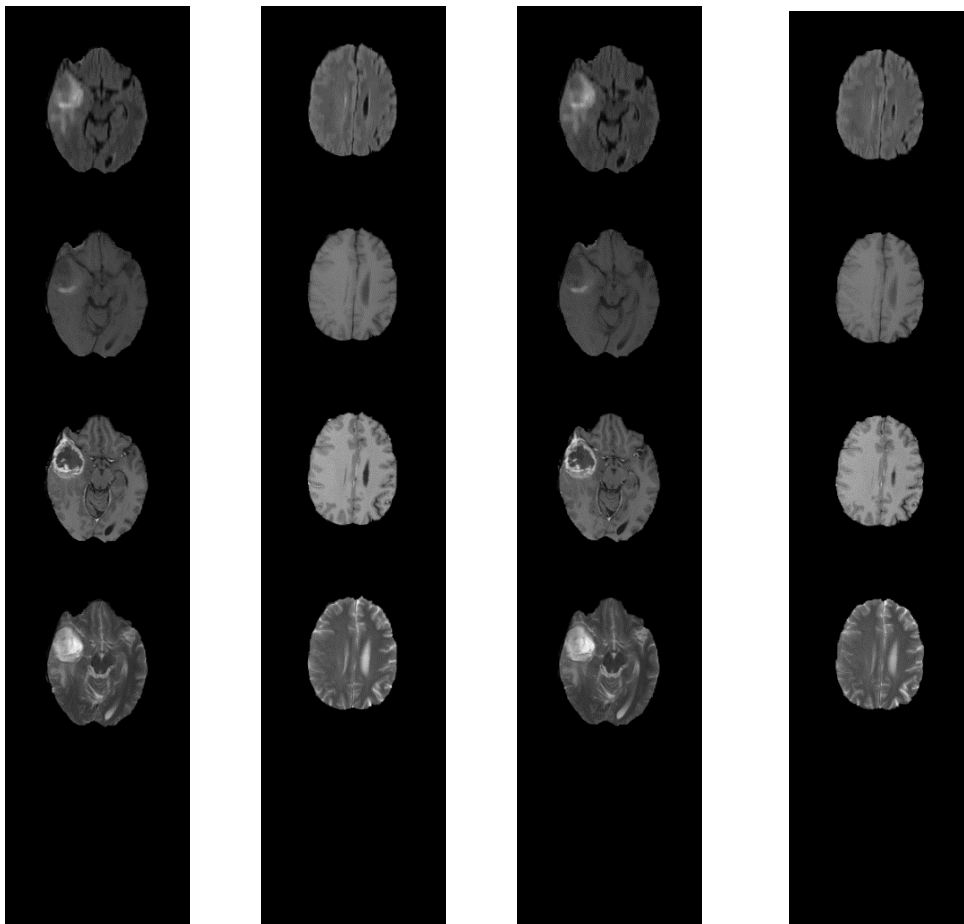


Figure 4.1 BRATS 2015 Dataset snaps

4.2 Implementation of robust U-NET architecture

Gliomas brain tumors segmentation was tested using a variety of architectures, including modified U-NET architecture. Because most patches belong to classes 0 and 1, we also employed a two-phase training model to lessen the influence of the class imbalance problem. We used their true ratio in the dataset to train the model in the first step. The network was then trained again with an

equal number of patches from each class, using the prior training results. Experimenting with this strategy, we discovered that it improved network performance by 1%.

4.2.1 Designed Modified U-NET architecture

To begin our segmentation attempts, we used U-NET as our baseline models. Although U-NET is an older architecture, we updated it in the sense that we employed the most recent trend in CNN, namely the regularization layer, hyper parameter adjustment, and two-phase training, to improve segmentation results.

The implementation is carried out on scans of 220 HHG and 54 LGG gliomas brain tumors. Because the dataset is in 3-D and the BRATS dataset lacks resolution in the third dimension, we converted the 3-D data into a 2-D image dataset before starting the training procedure. The network is trained over a period of 50 epochs on a total of ten thousand patches. On two phases, we also saw the implementation of our modified VGG architecture.

In terms of segmenting the gliomas tumors, the proposed model performed admirably. It was discovered that by utilizing a dropout layer network, it was possible to train more effectively. As a result, there was less over fitting in the training.

Our proposed U-NET Architecture appears to operate well based on the results, since it learns good local and global features during the training. We used 65 epochs to train our suggested network for a total of ten thousand training patches. We observed that there is no benefit to training beyond 65 epochs, and the network has already reached convergence.

4.3 Step by Step Training mechanism

The majority of the brain imaging pixels in gliomas tumors segmentation datasets are healthy tissues, resulting in an unbalanced class distribution. To properly learn data, the model should train a large number of patches from each class. This is not the case with the standard one-phase training method. We also noticed that when the number of feature maps rises, the likelihood of over fitting increases dramatically, and if the feature is greatly reduced, the network underfits. As a result, the dropout value of 0.4 is changed to eliminate the training's weak feature.

Because the fully connected layer consumes the majority of the time during network training, an optimal size of 1024 completely connected (FC) features was selected to achieve stability.

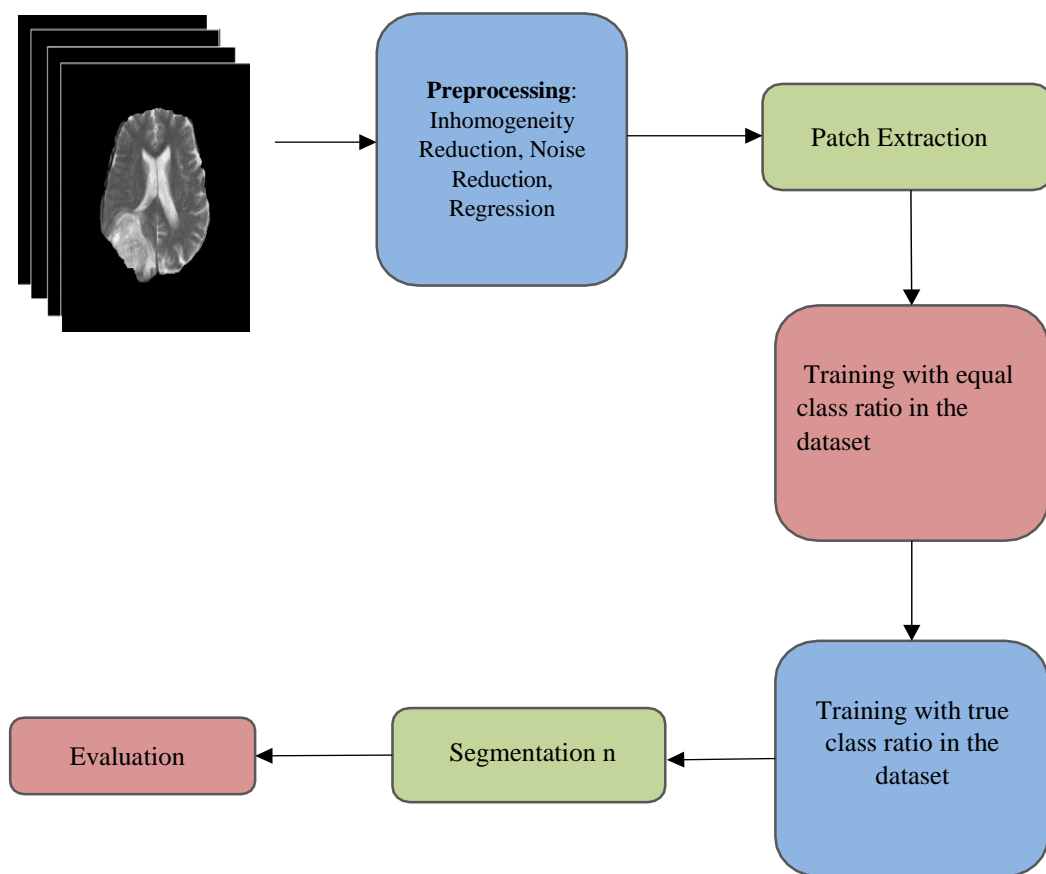


Figure 4.2 Complete overview of Training mechanism

4.4 Testing phase

In the BRATS 2015 dataset, there are 1000 test photos. Before sending the test image to the network, the photos are processed using the same image processing technique. To execute testing, the 3-D test data is transformed to 2D and then preprocessed. Intensity Normalization and N4ITK bias field correction techniques are used as pre-processing procedures. On our machine, the testing process takes about 4-5 minutes to get findings. The test findings were evaluated using three parameters: Dice Coefficient, Sensitivity, and Specificity.

Ground Truth and Detections
GT=green, pred=red, captions: score/loU

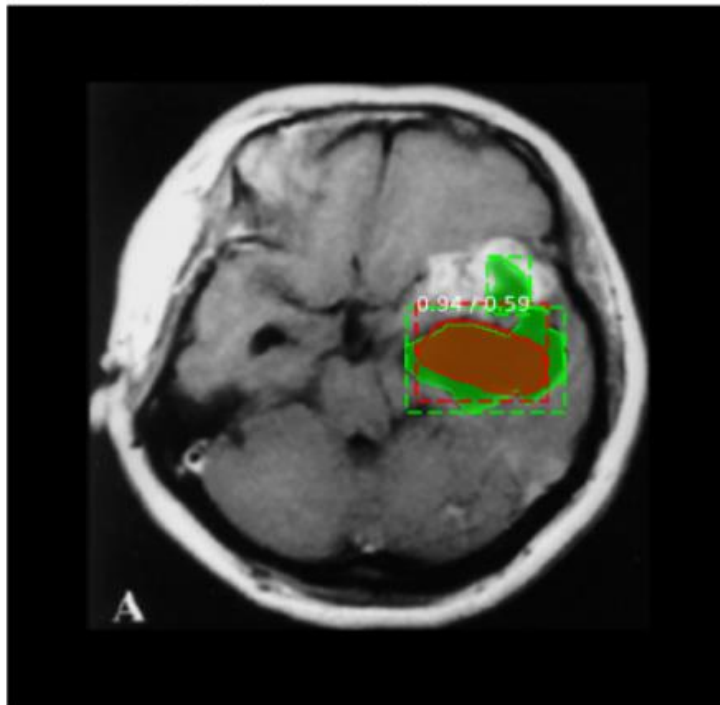


Figure4.3 Segmented output

Ground Truth and Detections
GT=green, pred=red, captions: score/loU

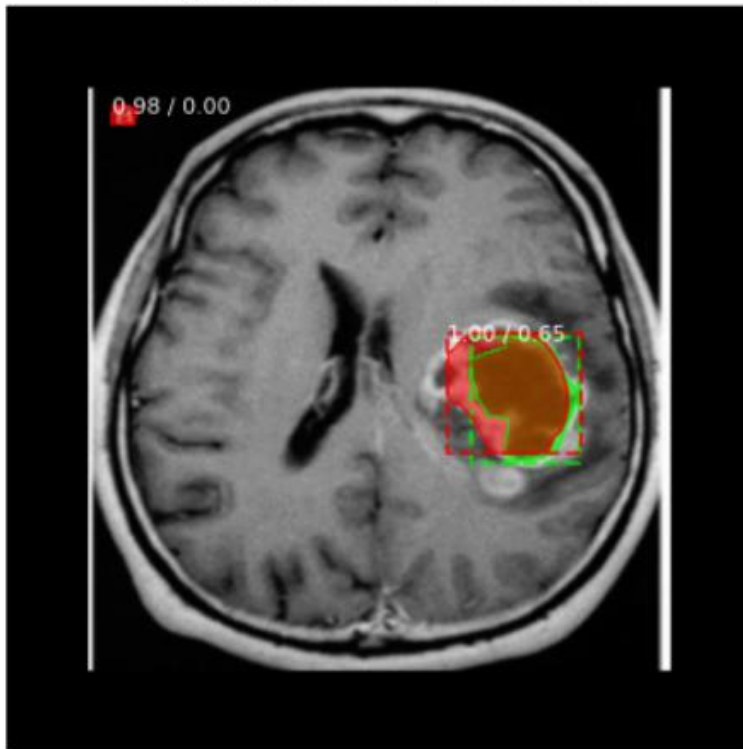


Figure 4.4 Segmented output 2

4.5 Detail overview of hardware

The area of machine learning obtained a big performance boost with the introduction of high-performance graphics processing units (GPUs), because deep learning techniques necessitate a large amount of matrix multiplication, which GPUs made possible. ImageNet [46] relied heavily on the availability of high-performance GPUs and their CUDA API. Prior to the introduction of modern GPUs, graphic performance was solely dependent on the CPU's capability. The performance of early NVIDIA GPUs was up to 70 times higher than that of conventional personal computers.

- Architecture was trained using Core-i9 9th Gen. Linux mint machine with RTX 2080 11 GB graphics card and 64 GB RAM and 1TB SSD.
- The primary language used was Python.
- NumPy and SciPy were used for the vast majority of numerical computations.
- Scikit learn was used for the machine learning algorithms.
- All deep learning related code was written using Keras, with a backend of TensorFlow.

4.6 Fine tuning of hyper-parameter of U-NET architecture

We used the Keras [47] library with Tensor Flow as the back-end to develop our framework on an Ubuntu computer. Four 33*33 pixel images are fed into the network as input. During training, batches of 64 and 128 were used.

We trained the model until it reached convergence. In our model, we used a max and average pooling layer. While max pooling is implemented in both networks, the last pooling layer in the proposed U-NET architecture is global average pooling. The pooling and convolution stride sizes are both fixed at 2.

4.6.1 Neuronal Activation

After each layer, an activation function is utilized to modulate the output values of the neurons. Linear, Tangent (tanh), sigmoid Rectified Linear unit (ReLU), leaky ReLU, and max-out are some of the activation layers proposed by researchers to manage the value of neurons. A value between [-1,1] is produced by the tangent activation function. The ReLU activation function is a nonlinear activation function that returns either a 0 or a 1.

4.6.2 Activation Functions

To monitor the output values of a neuron after each layer, an activation mechanism is used. The researchers have suggested several activation layers to regulate the importance of the neuron, i.e the tangent activation function returns a value between $[-1,1]$. Linear, Tangent (tanh), sigmoid Rectified Linear Unit (ReLU) and leaky ReLU, and max-out. The activation function of ReLU is a nonlinear activation function which generates either a zero or a positive value.

4.6.3 Normalization

To normalize each layer from the input data, we used Batch Normalization (BN) [48]. Batch normalization uses an activation feature to regulate the mean and standard of the function, close to 0 and 1 deviation respectively. Because of the high learning rate, layer weights often change radically, allowing the minor shifts to enhance results in inadequate resources. During back-propagation, BN regulates the gradient within an appropriate range.

4.6.4 Loss function Optimizers

The loss function value at the output of the network is calculated by an optimizer and these modified values are propagated back to the network to refine the preparation. In order to accelerate, we analyzed different optimizers in our network. We taught the network to fine-tune our outcome with three loss function optimizers. First of all, we used stochastic gradient descent (SGD), which is commonly known as the default optimizer. We then further played with our Adam optimizer network.

4.7 Comparative analysis of results

Table 4 presents a comprehensive comparative analysis on brain tumor segmentation of different techniques applied on BRATS dataset up till now. From year 2015 to 2021, we listed all the proposed methodology their results in term of dice score and datasets they used. In the end we listed our proposed framework with highest achieved dice score.

TABLE 4.1 Comparative analysis using Dice score as performance evaluating of various brain tumor segmentation architectures

| Num. | Writer of the paper | Architecture | Published in | Menu-driven interface | Dice score | Datasets | Reference |
|-----------|-----------------------------------|-------------------------------------|--------------|-----------------------|-------------|--------------------|-----------|
| 1 | E. Abdel-Maksoud | Fuzzy c-mean and k-mean clustering | 2015 | Automatic | 0.85 | DICOM | [16] |
| 2 | N. J. Tustison | Conventional Machine Learning | 2015 | Automatic | 0.86 | BRATS 2013 | [17] |
| 4 | I. Njeh, et al. | A Graphic matching approach | 2015 | Semi-auto | 0.76 | BRATS 2012 | [18] |
| 5 | Pereira et al. | CNN architecture | 2016 | Automatic | 0.88 | BRATS 2015 | [8] |
| 5 | Mohammad, et al | CNN two phase training architecture | 2016 | Automatic | 0.88 | BRATS 2013 | [9] |
| 6 | Huber, T, et al | Conventional processing algorithms | 2015 | Semi-automatic | 0.86 | 3-D MPRAGE-private | [19] |
| 7 | M. Soltaninejad | Super pixel based Classification | 2017 | Automatic | 0.87 | BRATS 2015 | [20] |
| 8 | S. Amiri et al. | Support vector algorithms | 2016 | Automatic | 0.84 | BRATS 2012 | [21] |
| 9 | J. Liu, et al. | Neural Network | 2018 | Automatic | 0.88 | 3-D MPRAGE-private | [32] |
| 10 | D. Liu, H. Zhang. | Deep neural networks | 2018 | Automatic | 0.88 | BRATS 2015 | [14] |
| 11 | Proposed Mohsin jabbar | U-NET with modification | 2021 | Automatic | 0.92 | BRATS 2015 | |

Chapter 5: Conclusion and Future Work

5.1 Conclusion

Due to high class imbalance of brain MRI images it is very difficult task to segment properly of brain tumor and aim is to predict tumors by segmenting the entire MRI images very carefully by adopting newly developed artificial intelligence. We proposed a novel framework named as U-NET with minor changes for gliomas tumor segmentation and achieved better result over all other frameworks up till now. Further, we discussed in detail all the available dataset with their challenges and works on BRATS 2015 dataset challenge. All the segmentation and classification techniques divided into four sub categories such as conventional image processing, deep neural networks, conventional and clustering Machine learning methods. In all of these methods, deep learning methods give better results with high time constraints and slow processing time.

To contribute the existing challenges and issues while in segmentation of brain tumors we proposed a U-NET novel architecture with minor changing in convolution layers such as adding pooling layers, activation function i.e. ReLU softmax for better precision in output layers. Further, we added image pre-processing session to increase the quality of the MRI images. Additionally, patch formation is also used for improving qualitative properties of the MRI input images. Each input image divided into multiples patch and these patches are extracted on the output side of the proposed architecture. After evaluation experimental results shows that our methodology works extraordinary well and achieve highest dice score on all the state-of-the-art frameworks present up till now.

As future directions, we should pay more attention by applying newly developed CNN models on different publicly available datasets and achieve better time constraint and high dice score. The filtration process in dataset can also be applied for betterment of result. Therefore, my research work paves the way towards new dimensions of the problem.

5.2 Future Work

Many improvements to the Glioma Brain Tumor Segmentation Process can be implemented for the feature goal

5.3 Dataset

The majority of automatic tumour segmentation methods have promising results in tumour segmentation and analysis; however, further improvements in these algorithms and the availability of additional image information from new image modalities may improve these methods and prove to be useful in the development of large-scale, clinically acceptable tumour segmentation methods. Because a larger dataset improves the performance of the Deep Convolutional Neural Network, more training instances should be added in the future for network training purposes. Another important factor to consider while creating a brain-tumor segmentation model is its resilience, or the ability of the algorithm to work with varied datasets. As a result, in order to create a reliable brain

tumour segmentation model, researchers should test their algorithm on a variety of datasets with varying modalities.

5.4 Transfer Learning

Transfer learning is a method in which a network learns information from one problem and applies it to another. We investigated transfer learning over the entire network training during our experiments. There are also some other transfer learning models that to provide excellent results. During fine-tuning, freezing the last layer of the network could be a good change in transfer learning technique. Fine tuning will be carried out in this manner on all layers of the network until it is fully integrated. The advantage of this method is that it reduces over fitting during the fine tuning process, which is an issue with our network as well.

Applying transfer learning to multiple medical datasets and then applying the learning outputs to the problem at hand could appear to yield superior results. Using transfer learning on the Brats dataset has some drawbacks. Because the BRATS dataset is a multimodality imaging dataset, network training comprises T1, T1C, T2, and Flair channels per input. However, when fine tuning, most datasets only have three channels or, in the case of grey level images, only one channel. A number of choices are available to deal with this issue. One option is to just turn off a channel.

To match the size of the feature channels, we trained on the BRATS dataset. New researchers are welcome to join this field of Glioma Brain Tumor Segmentation .

References

- Tocagen, tocagen.com/patients/brain-cancer/brain-cancer-statistics.
- Zacharaki, E. I., Wang, S., Chawla, S., Soo Yoo, D., Wolf, R., Melhem, E. R., & Davatzikos, C. (2009). Classification of brain tumor type and grade using MRI texture and shape in a machine learning scheme, *62*(6), 1609-1618.
- Ali I and Cem Direko. "Review of MRI-based brain tumor image segmentation using deep learning methods." (2016).
- Rao, B. Srinivasa and Dr. E. Sreenivasa Reddy. "A survey on Glioblastoma Multiforme Tumor Segmentation through MR images." (2016).
- R.K.-S. Kwan, A.C. Evans, G.B. Pike: "MRI simulation-based evaluation of image-processing and classification methods" *IEEE Transactions on Medical Imaging*. 18(11):1085–97, Nov 1999
- Valverde, Sergi et al. "Comparison of 10 brain tissue segmentation methods using revisited IBSR annotations." *Journal of magnetic resonance imaging: JMIR* 41 1 (2015): 93-101.
- Menze, Bjoern H., et al. "The Multimodal Brain Tumor Image Segmentation Benchmark (BRATS)." *IEEE Transactions on Medical Imaging*, vol. 34, no. 10, 2015, pp. 1993–2024., doi:10.1109/tmi.2014.2377694.
- Liew, Sook-Lei, et al. "A Large, Open Source Dataset of Stroke Anatomical Brain Images and Manual Lesion Segmentations." *Scientific Data*, vol. 5, 2018, p. 180011., doi:10.1038/sdata.2018.11.
- O. Commowick, F. Cervenansky, R. Ameli, *MSSEG Challenge Proceedings: Multiple Sclerosis Lesions Segmentation Challenge Using a Data Management and Processing Infrastructure* (2016).
- I. Išgum, M. J. Benders, B. Avants, M. J. Cardoso, S. J. Counsell, E. F. Gomez, L. Gui, P. S. H"uppi, K. J. Kersbergen, A. Makropoulos, et al., Evaluation of automatic neonatal brain segmentation algorithms: the NeoBrainS12 challenge, *Medical image analysis* 20 (1) (2015) 135–151.
- A. M. Mendrik, K. L. Vincken, H. J. Kuijf, M. Breeuwer, W. H. Bouvy, J. De Bresser, A. Alansary, M. De Bruijne, A. Carass, A. El-Baz, et al., *MRBrainS challenge: online evaluation framework for brain image segmentation in 3T MRI scans*, *Computational intelligence and neuroscience* 2015.
- N. Sharma and L. M. Aggarwal, Automated medical image segmentation techniques, *Journal of Medical Physics/Association of Medical Physicists of India*, vol. 35, no. 1, p. 3, 2010.
- Dubey, Rash & Hanmandlu, Madasu & Gupta, S.K.. (2009). Semi- automatic Segmentation of MRI Brain Tumor. *ICGST-GVIP Journal*. 9.

D. L. Pham, C. Xu, and J. L. Prince, Current methods in medical image segmentation 1, Annual Review of Biomedical Engineering, vol. 2, no. 1, pp. 315-337, 2000

Huber, T, et al. "Reliability of Semi-Automated Segmentations in Glioblastoma." Clinical Neuroradiology, vol. 27, no. 2, pp. 153– 161,2015.

Albelwi, S.; Mahmood, A. A Framework for Designing the Architectures of Deep Convolutional Neural Networks. *Entropy* 19, 242,2017

Havaei, Mohammad, et al. "Brain Tumor Segmentation with Deep Neural Networks." Medical Image Analysis, vol. 35, 2017, pp. 18– 31.

Hussain, Saddam, et al. "Segmentation of Glioma Tumors in Brain Using Deep Convolutional Neural Network." Neurocomputing, vol. 282, 2018, pp. 248–261.

JKamnitsas, Konstantinos, et al. "Efficient Multi-Scale 3D CNN with Fully Connected CRF for Accurate Brain Lesion Segmentation." Medical Image Analysis, vol. 36, 2017, pp. 61–78.

D. Liu, H. Zhang, M. Zhao, X. Yu, S. Yao and W. Zhou, "Brain Tumor Segmentation Based on Dilated Convolution Refine Networks," 2018 IEEE 16th International Conference on Software Engineering Research, Management and Applications (SERA), Kunming, China, 2018, pp. 113-120.

S. Pereira, A. Pinto, V. Alves and C. A. Silva, "Brain Tumor Segmentation Using Convolutional Neural Networks in MRI Images," in IEEE Transactions on Medical Imaging, vol. 35, no. 5, pp. 1240-1251, May 2016.

K. Sudharani, T. Sarma, and K. S. Prasad, "Advanced Morphological Technique for Automatic Brain Tumor Detection and Evaluation of Statistical Parameters", vol. 24, pp. 1374-1387,

Jan. 2016.Top of Form

I. Zabir, S. Paul, M. A. Rayhan, T. Sarker, S. A. Fattah, and C. Shahnaz, "Automatic brain tumor detection and segmentation from multi-modal MRI images based on region growing and level set evolution", Jan. 2015

E. Abdel-Maksoud, M. Elmogy, and R. Al-Awadi, "Brain tumor segmentation based on a hybrid clustering technique", vol. 16, no. 1, pp. 71-81, Jan. 2015.

J. S. Cordova, "Quantitative Tumor Segmentation for Evaluation of Extent of Glioblastoma Resection to Facilitate Multisite Clinical Trials", vol. 7, no. 1, pp. 40-W5, Jan. 2014.

N. J. Tustison, "Optimal Symmetric Multimodal Templates and Concatenated Random Forests for Supervised Brain Tumor Segmentation (Simplified) with ANTsR", vol. 13, no. 2, pp. 209- 225, Jan. 2015.

M. Soltaninejad, "Automated brain tumour detection and segmentation using superpixel-based extremely randomized trees in FLAIR MRI", vol. 12, no. 2, pp. 183-203, Jan. 2017.

- S. Amiri, I. Rekik, and M. A. Mahjoub, "Deep random forest-based learning transfer to SVM for brain tumor segmentation", Jan. 2016.
- S. Xie, R. Girshick, P. Dollar, Z. Tu, and K. He, "Aggregated Residual Transformations for Deep Neural Networks", Jan. 2017.
- T. Raiko, H. Valpola, and Y. LeCun. "Deep learning made easier by linear transformations in perceptrons", In AISTATS, 2012.
- A. M. Saxe, J. L. McClelland, and S. Ganguli. 'Exact solutions to the nonlinear dynamics of learning in deep linear neural networks', 2013.
- J. Liu, "A Cascaded Deep Convolutional Neural Network for Joint Segmentation and Genotype Prediction of Brainstem Gliomas", vol. 65, no. 9, pp. 1943-1952
- I. Njeh, "3D multimodal MRI brain glioma tumor and edema segmentation: A graph cut distribution matching approach", vol. 40, pp. 108-119, Jan. 2015. 2018f
- P. Charles, Project title, 2013, (<https://github.com/charlespwd/project-title>).
- Prastawa M, Bullitt E, Gerig G. "Simulation of brain tumors in mr images for evaluation of segmentation efficacy", *Medical Image Analysis*,13(2):297- 311.2009
- I. Njeh, "3D multimodal MRI brain glioma tumor and edema segmentation: A graph cut distribution matching approach", vol. 40, pp. 108-119, Jan. 2015. 2018
- N. J. Tustison, B. B. Avants, P. A. Cook, Y. Zheng, A. Egan, P. A. Yushkevich, et al., "N4ITK: improved N3 bias correction," *IEEE transactions on medical imaging*, vol. 29, pp. 1310-1320, 2010.
- S. Pieper, B. Lorensen, W. Schroeder, and R. Kikinis, "The NA-MIC Kit: ITK, VTK, pipelines, grids and 3D slicer as an open platform for the medical image computin

community," in *Biomedical Imaging: Nano to Macro, 2006. 3rd IEEE International Symposium on*, 2006, pp. 698-701

A. Fedorov, R. Beichel, J. Kalpathy-Cramer, J. Finet, J.-C. Fillion-Robin, S. Pujol, *et al.*, "3D Slicer as an image computing platform for the Quantitative Imaging Network," *Magnetic resonance imaging*, vol. 30, pp. 1323-1341, 2012.

A. Krizhevsky, I. Sutskever, and G. E. Hinton, "Imagenet classification with deep convolutional neural networks," in *Advances in neural information processing systems*, 2012, pp. 1097-1105.

S. Dieleman, K. W. Willett, and J. Dambre, "Rotation-invariant convolutional neural networks for galaxy morphology prediction," *Monthly notices of the royal astronomical society*, vol. 450, pp. 1441-1459, 2015

E. Shelhamer, J. Long, and T. Darrell, "Fully convolutional networks for semantic segmentation," *IEEE transactions on pattern analysis and machine intelligence*, 2016.

I. J. Goodfellow, D. Warde-Farley, M. Mirza, A. C. Courville, and Y. Bengio, "Maxout Networks," *ICML (3)*, vol. 28, pp. 1319-1327, 2013

G. W. Burr, R. M. Shelby, S. Sidler, C. Di Nolfo, J. Jang, I. Boybat, *et al.*, "Experimental demonstration and tolerancing of a large-scale neural network (165 000 synapses) using phase-change memory as the synaptic weight element," *IEEE Transactions on Electron Devices*, vol. 62, pp. 3498-3507, 2015

S. Xie, R. Girshick, P. Dollar, Z. Tu, and K. He.: Aggregated Residual Transformations for Deep Neural Networks, Jan. 2017.

C. K. D. Z. R. S. R. L. G. P. A. Schlögl, "A fully automated correction method of EOG artifacts in EEG recordings.," *Clin.Neurophys*, pp. 118(1):98-104., 2007

P. Charles, Project title, 2013, (<https://github.com/charlespwd/project-title>

S. Ioffe and C. Szegedy, "Batch normalization: Accelerating deep network training by reducing internal covariate shift," *arXiv preprint arXiv:1502.03167*, 2015

N. H. G. K. A. S. I. & S. R. Srivastava, "Dropout: A Simple Way to Prevent Neural Networks from Overfitting," *Journal of Machine Learning Research*, , vol. <http://doi.org/10.1214/12AOS1000> , no. 15, p. 1929–1958., 2014.

N. Srivastava, G. E. Hinton, A. Krizhevsky, I. Sutskever, and R. Salakhutdinov, "Dropout: a simple way to prevent neural networks from overfitting," *Journal of Machine Learning Research*, vol. 15, pp. 1929-1958, 2014.

<https://medium.com/@sh.tsang>. (2018, September 10). Review: Inception-v3—1st Runner Up (Image Classification) in ILSVRC 2015. Medium. Retrieved February 27, 2019, from

<https://medium.com/@sh.tsang/review-inception-v3-1st-runner-up-image-classification-in-ilsvrc-2015-17915421f77c>.

- [1] B. H. Menze, A. Jakab, S. Bauer, J. Kalpathy-Cramer, K. Farahani, J. Kirby, *et al.*, "The multimodal brain tumor image segmentation benchmark (BRATS)," *IEEE transactions on medical imaging*, vol. 34, pp. 1993-2024, 2015.
- [2] B. H. Menze, A. Jakab, S. Bauer, J. Kalpathy-Cramer, K. Farahani, J. Kirby, *et al.*, "The multimodal brain tumor image segmentation benchmark (BRATS)," *IEEE transactions on medical imaging*, vol. 34, pp. 1993-2024, 2015

ABBREVIATION

DCNN: Deep Convolutional Neural Network

BRATS: Brain Tumor Segmentation Challenge

MRI: Magnetic Resonance Imaging

CAD: Computer Aided Diagnosis

CNN: Convolutional Neural Network

GT: Ground Truth

LGG: Low Grade Glioma

HGG: High Grade Glioma

CT: Computed Tomography

PET: Position Emission Tomography

SPECT: Single Photon Emission Computed Tomography

NMR: Nuclear Magnetic Resonance

MRS: Magnetic Resonance Spectroscopy

EEG: Electroencephalography

WM: White Matter

SVM: Support Vector Machine

GM: Gray Matter

FCM: Fuzzy C-Means

KIFCM: called k-mean integrated with fuzzy C-mean clustering

IRT: Infrared thermography

DICOM: Digital Imaging and Communications in Medicine

ILSVRC: ImageNet Large Scale Visual Recognition Competition

N4ITK: Improved N3 Bias Correction

FLAIR: Fluid-attenuated inversion recovery

ISBR: Internet Brain Segmentation Repository

DCR: Dilated convolution refined

ROI: Region of Interest

TP: True Positive

TN: True Negative

FP: False Positive

FN: False Negative

ReLU: rectified linear unit

DNN: Deep Neural Network CSF: Cerebrospinal Fluid

MEG: Magnetoencephalography DF: Decision Forests

RF: Random Forests

SGD: Stochastic Gradient Descent GPU: Graphical Processing Unit DSC: Dice Similarity Coefficient SR: Sparse Representation

ERT: extremely randomized trees RDF: Random Decision Forests CPU: Central Processing Unit

PCA: Principle Component Analysis VGG: Visual Geometry Group

FC: Fully Connected

CUDA: Compute Unified Device Architecture API: application program interface

BN: Batch Normalization TL: Transfer Learning PC: Personal Computer DL: Deep Learning

GT: Ground Truth

SR: Sparse Representation RDF: Random Decision Forests